Spin-wave modes of ferromagnetic films

R. E. Arias

Departamento de Física, CEDENNA, Facultad de Ciencias Físicas y Matemáticas, Universidad de Chile, Santiago, Chile

(Received 18 November 2015; revised manuscript received 14 September 2016; published 10 October 2016)

The spin-wave modes of ferromagnetic films have been studied for a long time experimentally as well as theoretically, either in the magnetostatic approximation or also considering the exchange interaction. A theoretical method is presented that allows one to determine with ease the exact frequency dispersion relations of dipole-exchange modes under general conditions: an obliquely applied magnetic field, and surface boundary conditions that allow for partial pinning, which may be of different origins. The method is a generalization of Green's theorem to the problem of solving the linear dynamics of ferromagnetic spin-wave modes. Convolution integral equations for the magnetization and the magnetostatic potential of the modes are derived on the surfaces of the film. For the translation-invariant film these become simple local algebraic equations at each in-plane wave vector. Eigenfrequencies result from imposing a 6×6 determinant to be null, and spin-wave modes follow everywhere through solving linear 6×6 inhomogeneous systems. An interpretation of the results is that the Green's functions represent six independent plane-wave solutions to the equations of motion, with six associated complex perpendicular wave vectors: volume modes correspond to the cases in which two of these are purely real at a given frequency. Furthermore, the convolution extinction equations enforce the boundary conditions: this is possible at specific eigenfrequencies for a given in-plane wave vector. Magnetostatic modes may also be obtained in detail. At low frequencies and for some obliquely applied magnetic fields, magnetostatic and dipole-exchange volume modes may have forward or backward character depending on the frequency range.

DOI: 10.1103/PhysRevB.94.134408

I. INTRODUCTION

A very important geometry in practical applications of modern ferromagnetism corresponds to thin films. It is a preferred geometry of sample preparation, whether in isolation or as part of multilayer devices. Indeed, many important experimental discoveries and applications in magnetism and related areas have been accomplished in ferromagnetic thin films. In particular, the number of applications in which spin waves in thin ferromagnetic films are relevant is large, and still counting: ferromagnetic films have been important in the past, and most probably still for many years to come.

Thus, a matter of interest is, and has been, to determine the frequencies and nature of dipole-exchange spin-wave modes that can propagate in thin films, both from the experimental and theoretical points of view. For these modes the dipolar and the exchange interactions are both relevant, which typically occurs at length scales of the order of nanometers. The study of dipole-exchange spin-wave modes in thin films was preceded by that of magnetostatic modes, which propagate in films of thicknesses typically in the range of micrometers [1,2] where retardation effects and the influence of exchange may be neglected. Later, dipole-exchange modes were studied theoretically within a continuum theory that applies for wavelengths over the exchange length scale of the given ferromagnet, which is of the order of nanometers. In order to obtain the linear spin-wave modes within the continuum approach one needs to solve the Landau-Lifshitz (LL) equations of motion for the magnetization in their linear version, together with the determination of the associated demagnetizing fields (the latter involve electromagnetic boundary conditions, and one also needs to apply exchange boundary conditions on the surfaces of the film). This subject has been studied for a long time now (it has been reviewed from the theoretical point of view in Ref. [3]). According to Ref. [4] the theoretical studies of dipole-exchange modes may be classified into two groups. The first group, or partial-wave approach (PW), corresponds to representing the magnetization and magnetostatic potential in terms of an appropriate set of plane-wave solutions and then solving with this set the LL equations and magnetostatic equations subject to electrodynamic and exchange boundary conditions. A representative set of references of the PW group is [5–15]. The second group, or spin-wave mode approach (SWM), uses an integral representation for the demagnetizing field in terms of the magnetization (it satisfies the electromagnetic boundary conditions), and when replaced in the LL equation of motion this becomes an integro-differential equation. The latter equation is solved by writing the magnetization as an infinite series in terms of basis vector functions that satisfy the exchange boundary conditions (spin-wave modes): the eigenfrequencies result from imposing an infinite determinant to be null. Representative references that have followed the SWM approach are [16–21]. Among these works we particularly mention Ref. [19], which would be the standard theoretical reference for dipole-exchange modes under an applied magnetic field of arbitrary direction and boundary conditions with variable pinning. This reference provides approximate formulas for the dispersion relation of the modes by neglecting nondiagonal terms of the eigenvalue problem involved. In the present work we tested these approximate formulas in two particular cases: in one they work well except for the fact that they do not describe well regions where modes hybridize, but in another case they do not describe well the exact dispersion relations; thus we conclude that they must be used with care. Also, in their work it requires a deal of care to analyze regions where surface and volume modes hybridize: indeed its implementation is not simple; a perturbation theory was developed in order to take into account in these regions the effect of nondiagonal terms. Within this approach numerical solutions of these very large eigenvalue problems with full matrices may be undertaken in order to determine the dipole-exchange modes

with precision: this has been done for example in Ref. [20], where also the effect of volume anisotropy in the spin waves was investigated. Furthermore, all the previously mentioned works on the PW and SWM approaches did study theoretically the dipole-exchange modes within a linear approximation, but these modes have also been studied within a nonlinear context, for example as in Ref. [22].

Within micromagnetic linear spin-wave theory the present study presents exact theoretical results for the dipole-exchange modes of a thin ferromagnetic film that allow one to simply determine their frequencies and their shapes. It is a different approach to those previously mentioned, i.e., PW and SWM, although it will be seen that it ends up being closer to the PW approach. The theory is based on a set of convolution integral equations for the modes and their frequencies: a set of homogeneous eigenvalue equations. It is a generalization of Green's theorem to the case of dipole-exchange modes, i.e., to solving the Landau-Lifshitz equations for the magnetization dynamics of the modes coupled with the calculation of their associated demagnetizing and exchange fields. For a ferromagnetic thin film modeled as infinite in-plane, due to translational invariance these convolution integral equations written in Fourier space become simple local algebraic eigenvalue equations for the amplitudes of the modes at the surfaces and for their frequencies, at a given in-plane wave vector of interest. These results are obtained for an arbitrary direction of an applied magnetic field, and also for boundary conditions of partial pinning [23] on the surfaces, as was originally done in Ref. [19]. The frequencies at a given in-plane wave vector can be determined imposing the determinant of a 6×6 matrix to be null [Eqs. (45), (46)]; this corresponds to the solution of a homogeneous system of equations: with modern computers and mathematical software it is almost instantaneous to draw frequency dispersion curves of the spin-wave modes of a ferromagnetic film. Then, to obtain the associated shapes of the modes everywhere is a simple task: one needs to solve a linear 6×6 inhomogeneous problem. There is the possibility also of considering more general boundary conditions than those of Ref. [19]: they may be chosen differently in both film surfaces and they may represent tensorial surface anisotropies or boundary conditions of more modern interest such as exchange bias [24] and the Dzyaloshinskii-Moriya interaction [25]. We mainly considered our film to be in contact with nonmagnetic media, but we also establish equations applicable to surfaces in contact with ideal metals.

We also present the analogous theory for magnetostatic modes: it is an alternative practical method to determine the frequencies and shapes of magnetostatic modes under an applied magnetic field of arbitrary direction. The latter method provides a way to check the long-wavelength limit of the previous theory for dipole-exchange modes, and it also allows one to better understand the structure of the dispersion relations of the dipole-exchange modes, in particular in relation with the role of the surface modes that have a dipolar origin. A thorough interpretation of the magnetostatic spin-wave modes is possible and guides the more complex analysis of dipole-exchange modes.

Further interpretation of the dipole-exchange modes is possible. In particular the origin, number, and type of dispersion relations of the dipole-exchange volume modes are understood. The Green's functions at specific frequencies may be interpreted as six independent plane-wave solutions of the equations of motion with associated perpendicular wave vectors that are in general complex numbers. Volume modes occur when two of these six plane-wave solutions have purely real perpendicular wave vectors at given frequencies (for oblique orientations of the applied magnetic fields these two real perpendicular wave vectors have different signs and magnitudes, while for the simpler parallel and perpendicular orientations they have different signs but equal magnitudes). The convolution extinction equations that the method provides for the modes evaluated at the surfaces effectively enforce the boundary conditions, something that is possible at specific eigenfrequencies associated with given in-plane wave vectors; i.e., one obtains the dispersion relations of the modes.

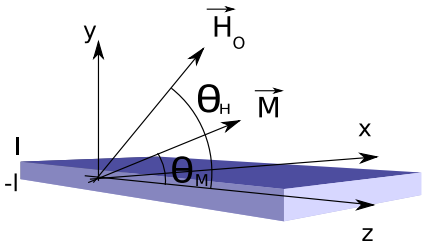

FIG. 1. Geometry of the ferromagnetic thin film, applied magnetic field at an angle θ_H from the plane, and resulting equilibrium magnetization at an angle θ_M from the plane.

II. DIPOLE EXCHANGE MODES OF FERROMAGNETIC THIN FILMS

The equations to be solved in order to obtain the dipole-exchange spin-wave modes of a thin ferromagnetic film under an inclined applied magnetic field are described in the following. These are micromagnetic equations; i.e., the magnetization dynamics is modeled in terms of continuous fields (approximation valid over the exchange length scale, which in general is of the order of nanometers), and they are solved in the linear approximation.

A. Equilibrium magnetization configuration and linear deviations

We proceed to describe the geometry of the thin film, the generally inclined applied magnetic field, the equilibrium configuration, and linear dynamic deviations from it. The geometry of the ferromagnetic thin film and the selected coordinate axis are shown in Fig. 1.

An applied magnetic field of magnitude H_0 is considered to be applied in a direction that makes an angle θ_H with respect to the $\hat{z}$ direction, which is parallel to the plane of the film. Thus, the equilibrium magnetization will be inclined at an angle θ_M with respect to the plane ($\theta_M < \theta_H$), defining the $\hat{\vec{z}}$ direction, i.e., $\vec{M}_{eq} = M_s \hat{\vec{z}}$. This inclined magnetization has an associated internal magnetic field $\vec{H}_i = H_0 \cos\theta_H \hat{z} + (H_0 \sin\theta_H - 4\pi M_s \sin\theta_M)\hat{y} = H_i \hat{\vec{z}}$, i.e., along the $\hat{\vec{z}}$ direction, showing that in equilibrium the magnetization and the internal magnetic field are parallel. These angles θ_M,θ_H are related

through

$$\frac{\sin\theta_M}{\cos\theta_M} = \frac{H_0\sin\theta_H - 4\pi M_s\sin\theta_M}{H_0\cos\theta_H}. \quad (1)$$

The linear dipole-exchange normal modes are eigensolutions of the Landau-Lifshitz equations for the linear magnetization dynamics coupled with the magnetostatic equations that determine the associated dipolar fields (the magnetization satisfies appropriate boundary conditions on the film surfaces; in our case we will consider partially pinned boundary conditions). To linear approximation the magnetization is expanded as

$$\vec{M}(\vec{x},t) \simeq M_s\hat{\vec{z}} + \vec{m}(\vec{x},t) = M_s\hat{\vec{z}} + m_x(\vec{x},t)\hat{x} + m_{\tilde{y}}(\vec{x},t)\hat{\tilde{y}}, \quad (2)$$

with $\hat{\tilde{y}}$ and $\hat{x}$ directions perpendicular to the equilibrium magnetization direction $\hat{\vec{z}}$. We will look for linear eigenmodes of frequency ω, i.e., $\vec{m}(\vec{x},t) = \mathrm{Re}[\vec{m}^{\omega}(\vec{x})\exp(-i\omega t)]$.

B. Magnetostatic equations

The spin-wave normal modes generate dynamic demagnetizing fields that satisfy the following magnetostatic equations:

$$\nabla\cdot\vec{b}^{\omega} = 0, \quad \nabla\times\vec{h}_D^{\omega} = 0, \quad (3)$$

with $\vec{b}^{\omega}$ and $\vec{h}_D^{\omega}$ the magnetic induction and demagnetizing fields, respectively; $\vec{b}^{\omega} = \vec{h}^{\omega} + 4\pi\vec{m}^{\omega}$. It follows that the demagnetizing field of the modes can be written in terms of a magnetostatic potential, i.e., $\vec{h}_D^{\omega} = -\nabla\phi^{\omega}$, inside and outside the sample. Outside the sample $\vec{b}^{\omega} = \vec{h}_D^{\omega}$, and it satisfies the equation

$$0 = \nabla\cdot\vec{b}^{\omega} = -\nabla^2\phi^{\omega}. \quad (4)$$

Inside the sample $\vec{b}^{\omega} = \vec{h}_D + 4\pi\vec{m}^{\omega}$, and it satisfies the equation

$$0 = \nabla\cdot\vec{b}^{\omega} = \nabla\cdot\vec{h}_D^{\omega} + 4\pi\nabla\cdot\vec{m}^{\omega}, \quad (5)$$

which is equivalent to the following equation for the magnetostatic potential:

$$-\nabla^2\phi^{\omega} + \frac{1}{2}\left[\left(\frac{\partial}{\partial x} - i\frac{\partial}{\partial\tilde{y}}\right)M_+^{\omega} + \left(\frac{\partial}{\partial x} + i\frac{\partial}{\partial\tilde{y}}\right)M_-^{\omega}\right] = 0, \quad (6)$$

where the following definitions were introduced: $m_{\pm} \equiv m_x \pm i m_{\tilde{y}} \equiv M_{\pm}/4\pi$. The magnetostatic equations are to be solved with their associated boundary conditions, which are continuity of the normal component of $\vec{b}^{\omega}$ and the tangential component of $\vec{h}^{\omega}$ (or equivalently continuity of the magnetostatic potential ϕ^{ω}).

C. Landau-Lifshitz equation and pinning conditions

The Landau-Lifshitz equation for the magnetization dynamics corresponds to

$$\frac{d\vec{M}}{dt} = -|\gamma|\vec{M}\times\vec{H}_{\mathrm{eff}}(\vec{M}), \quad (7)$$

with $|\gamma|$ the absolute value of the gyromagnetic factor, and the effective field, $\vec{H}_{\mathrm{eff}}(\vec{M})$, is the sum of the applied field, the demagnetizing field, and the exchange field:

$$\vec{H}_{\mathrm{eff}}(\vec{M}) = H_0(\cos\theta_H\hat{z} + \sin\theta_H\hat{y}) + \vec{H}_D(\vec{M}) + (D/M_s)\nabla^2\vec{M}, \quad (8)$$

with D the exchange stiffness constant, $D = 2A/M_s$. Thus, replacing Eq. (2) in Eq. (7), the Landau-Lifshitz equation for the linear modes takes the form

$$i\omega\vec{m}_{\omega} = \hat{\vec{z}}\times|\gamma|(D\nabla^2\vec{m}_{\omega} - M_s\nabla\phi_{\omega} - H_i\vec{m}_{\omega}). \quad (9)$$

We consider the possibility of uniaxial surface anisotropy in the surfaces of the film, with $U_{an}^s = K_s[1 - (\vec{M}\cdot\vec{n}/M_s)^2]$ the surface anisotropy areal energy density ($\hat{n}$ is the unitary vector normal to the surface, pointing to the exterior of the sample). For a film with uniaxial surface anisotropy Soohoo [23] derived the following form of the pinning conditions (in our case the sign of K_s differs from that reference):

$$0 = \frac{\partial m_{\tilde{y}}}{\partial n} - \lambda\cos(2\theta_M)m_{\tilde{y}}, \quad (10)$$

$$0 = \frac{\partial m_x}{\partial n} + \lambda\sin^2(\theta_M)m_x, \quad (11)$$

with $\lambda = 2K_s/DM_s$ (see also Refs. [26,27]), $n = y$ in the upper surface of the film, and $n = -y$ in the lower one. We refer to Eqs. (10) and (11) as the partially pinned boundary conditions (in our numerical calculations we considered that both surfaces have the same boundary conditions, which is not always the case in reality).

III. GREEN'S FUNCTIONS AND EXTINCTION EQUATIONS

The frequencies of the modes as well as their values on the surfaces of the sample will be obtained by solving integral equations satisfied by them. These are homogeneous extinction equations that may be thought of as a generalization of Green's theorem to the equations relevant to this case, i.e., the magnetostatic equations and the Landau-Lifshitz equation. This will require the introduction of some appropriate Green's functions, as indicated in the following.

A. Green's functions

1. Green's function outside the film

A Green's function appropriate for the medium outside the film satisfies the following equations ($\vec{b}_0 = -\nabla\phi_0$):

$$\nabla\cdot\vec{b}_0 = -\nabla^2\phi_0 = 4\pi\delta(\vec{x}-\vec{x}')\delta(t-t'). \quad (12)$$

A representation in Fourier space of this Green's function is introduced:

$$\phi_0(\vec{x}-\vec{x}';t-t') = \frac{1}{(2\pi)^2}\int d\omega e^{-i\omega(t-t')} \times \int dk e^{ik(z-z')}\phi_0^{(k,\omega)}(\vec{\rho}-\vec{\rho}'), \quad (13)$$

with $\vec{\rho} \equiv x\hat{x} + y\hat{y}$, and which leads to

$$\nabla\cdot\vec{b}_0^{\omega}(\vec{x}-\vec{x}') = 4\pi\delta(\vec{x}-\vec{x}'). \quad (14)$$

Consequently, $\phi_0^{(k,\omega)}$ satisfies:

$$(\nabla_\perp^2 - k^2)\phi_0^{(k,\omega)}(\vec{\rho}-\vec{\rho}') = -4\pi\delta(\vec{\rho}-\vec{\rho}'), \quad (15)$$

with $\vec{\rho} \equiv x\hat{x} + y\hat{y}$. A solution to this previous equation with the right singular behavior at the source is

$$\phi_0^{(k,\omega)}(\vec{\rho}-\vec{\rho}') = 2K_0(|k||\vec{\rho}-\vec{\rho}'|), \quad (16)$$

with K_0 a modified Bessel function of order zero. Close to the singularity, $K_0(|k|\rho) \simeq -\ln\rho$ for $\rho \to 0$, i.e., the right behavior associated with the delta function appearing in Eq. (15).

The Fourier transform with respect to the x direction of the previous result leads to

$$\phi_0^{(\vec{Q},\omega)}(\vec{\rho}-\vec{\rho}') = \frac{2\pi}{Q}\exp(-Q|y-y'|), \quad (17)$$

with $\vec{Q} \equiv q\hat{x} + k\hat{z}$ the in-plane wave vector, and $Q \equiv |\vec{Q}| = \sqrt{q^2+k^2}$ its magnitude.

2. *Interior Green's function*

The Green's function associated with the interior medium, when the source point ($\vec{x}'$) is outside the sample, satisfies the following equations ($\vec{b}_G^{\omega} = -\nabla\phi_G^{\omega} + 4\pi\vec{m}_G^{\omega}$):

$$\nabla\cdot\vec{b}_G^{\omega}(\vec{x}-\vec{x}') = 0, \quad (18)$$

$$i\omega\vec{m}_G^{\omega} = \hat{\vec{z}}\times|\gamma|\left(D\nabla^2\vec{m}_G^{\omega} - M_s\nabla\phi_G^{\omega} - H_i\vec{m}_G^{\omega}\right). \quad (19)$$

A simpler case of the previous equations for the Green's functions corresponds to the in-plane magnetized case, i.e., $\theta_M = 0$: there are three Green's functions (I, II, III), and they are detailed in Appendix A. For example, Green's function I takes the form

$$\phi_I^{-(k,\omega)} = CK_0(\beta_I|\vec{\rho}-\vec{\rho}'|), \quad (20)$$

$$M_\pm^{-(k,\omega)I} = K_\pm e^{\pm i\theta}K_1(\beta_I|\vec{\rho}-\vec{\rho}'|), \quad (21)$$

where β_I^2 satisfies a cubic equation and $C, K_\pm$ are constants that were determined [the previous forms of Eqs. (20) and (21) correspond to the case $\beta_I^2 > 0$, and θ represents the azimuthal angle of $\vec{\rho}-\vec{\rho}'$ in the x-y plane]. The associated Fourier transforms of the Green's functions of Eqs. (20) and (21) are

$$\phi_I^{-(\vec{Q},\omega)} = e^{-\sqrt{\beta^2+q^2}|y-y'|}/\sqrt{\beta^2+q^2}, \quad (22)$$

$$M_\pm^{-(\vec{Q},\omega)I} = ik_\pm e^{-\sqrt{\beta^2+q^2}|y-y'|}(q/\sqrt{\beta^2+q^2} \pm s), \quad (23)$$

with s the sign of $(y-y')$, and $k_\pm$ constants.

For the case of an arbitrary angle, the equations for the Green's functions (18) and (19) were written in Fourier space and based on the type of solutions (22) and (23); the solutions were found in the form

$$\phi_{G(u,d)}^{-(\vec{Q},\omega)} = A^{(u,d)}\exp(-\alpha^{(u,d)}|y-y'|),$$
$$M_\pm^{G(u,d)} = B_\pm^{(u,d)}\exp(-\alpha^{(u,d)}|y-y'|). \quad (24)$$

In these solutions (u,d) refer to regions where $s = \mathrm{sgn}(y-y') = (+,-)$, respectively. The $\alpha^{(u,d)}$ are roots of polynomials of sixth order in α that differ in the upper (u) and lower regions (d):

$$0 = \left[\left(\alpha_j^{(u,d)}\right)^2 - Q^2\right]\left\{d\left[\left(\alpha_j^{(u,d)}\right)^2 - Q^2\right] - h_i + \Omega\right\}\left\{d\right.$$
$$\times\left[\left(\alpha_j^{(u,d)}\right)^2 - Q^2\right] - h_i - \Omega\Big\} + \Big[\left(k\sin\theta_M\right.$$
$$\left.\left. \pm i\alpha_j^{(u,d)}\cos\theta_M\right)^2 + q^2\Big]\left\{d\left[\left(\alpha_j^{(u,d)}\right)^2 - Q^2\right] - h_i\right\}, \quad (25)$$

where $d \equiv D/4\pi M_s = l_{ex}^2$, with l_{ex} the exchange length, and $\Omega \equiv \omega/4\pi M_s|\gamma|, h_i \equiv H_i/4\pi M_s$ are the nondimensional frequency and magnitude of the internal field, respectively (in the $\pm$ signs, $+$ corresponds to α^u and $-$ to α^d). In each region one chooses three solutions with $\mathrm{Re}(\alpha) \geqslant 0$, each corresponding to a Green's functions set; i.e., the number of Green's functions is the same as for the case $\theta_M = 0$. Details are found in Appendix B.

B. Extinction equations

Integral equations are derived for the dipole-exchange normal modes using a generalization of Green's theorem that is appropriate for the equations satisfied by these modes. In particular, the Green's functions involved are evaluated with sources outside the regions of integration, leading to homogeneous or extinction equations.

1. *Extinction equation outside*

An extinction equation can be derived if one integrates in the region outside the sample the following expression that involves the Green's function outside the sample. The integrand is null; it follows from combining appropriately Eqs. (4) and (14) with the source point $\vec{x}'$ taken as an arbitrary point inside the sample:

$$\int_{V_{\mathrm{out}}} dV\left[\phi_0^{-\omega}(\vec{x}-\vec{x}')\nabla\cdot\vec{b}^{\omega}(\vec{x}) - \phi^{\omega}(\vec{x})\nabla\cdot\vec{b}_0^{-\omega}(\vec{x}-\vec{x}')\right] = 0. \quad (26)$$

Integrating by parts the previous equation, one obtains

$$\int_S d\vec{S}\cdot\left[\phi_0^{-\omega}(\vec{x}-\vec{x}')\vec{b}^{\omega}(\vec{x}) - \phi^{\omega}(\vec{x})\vec{b}_0^{-\omega}(\vec{x}-\vec{x}')\right] = 0, \quad (27)$$

with S the surface of the sample, with the convention that a surface element $d\vec{S}$ has a normal towards the outside of the sample.

For the geometry of a film the previous equation involves a convolution over the z and x axes, and since the Fourier transform of a convolution of two functions is the product of their Fourier transforms (evaluated with different signs of the wave vectors though), it leads to

$$0 = \phi_0^{-(\vec{Q},\omega)}(l-y')b_y^{(\vec{Q},\omega)}(l) - \phi^{(\vec{Q},\omega)}(l)b_{0y}^{-(\vec{Q},\omega)}(l-y')$$
$$-\phi_0^{-(\vec{Q},\omega)}(-l-y')b_y^{(\vec{Q},\omega)}(-l)$$
$$+\phi^{(\vec{Q},\omega)}(-l)b_{0y}^{-(\vec{Q},\omega)}(-l-y'). \quad (28)$$

Thus, conveniently the integral equations (27) have been transformed into simple algebraic equations, at specific values of the wave vector $\vec{Q}$. Due to the form of the Green's function of Eq. (17) in Eq. (28) there are terms proportional to $\exp(-Qy')$

and $\exp(Qy')$ for arbitrary y'; thus both terms should be null (y' belongs to the interior of the film, i.e., $-l < y' < l$). This leads to two simple equations for the modes:

$$0 = b_y^{(\vec{Q},\omega)}(l) - Q\phi^{(\vec{Q},\omega)}(l), \tag{29}$$

$$0 = b_y^{(\vec{Q},\omega)}(-l) + Q\phi^{(\vec{Q},\omega)}(-l). \tag{30}$$

2. *Extinction equation inside*

In order to obtain an extinction equation associated with the inside of the sample, we consider the following integral over the inside volume:

$$\int_{V_{\text{in}}} dV\left[\phi^{\omega}(\vec{x})\nabla\cdot\vec{b}_G^{-\omega}(\vec{x}-\vec{x}')-\phi_G^{-\omega}(\vec{x}-\vec{x}')\nabla\cdot\vec{b}^{\omega}(\vec{x})\right]=0, \tag{31}$$

which is null due to Eqs. (5) and (18) [notice that we have considered the Green's functions terms evaluated at $(-\omega)$, which will prove useful later; $\vec{x}'$ is a point outside the sample]. Integrating by parts Eq. (31), one obtains

$$\begin{aligned}0 = &\int_S d\vec{S}\cdot\left[\phi^{\omega}(\vec{x})\vec{b}_G^{-\omega}(\vec{x}-\vec{x}')-\phi_G^{-\omega}(\vec{x}-\vec{x}')\vec{b}^{\omega}(\vec{x})\right]\\ &-4\pi\int_{V_{\text{in}}} dV\left[\nabla\phi^{\omega}(\vec{x})\cdot\vec{m}_G^{-\omega}(\vec{x}-\vec{x}')\right.\\ &\left.-\nabla\phi_G^{-\omega}(\vec{x}-\vec{x}')\cdot\vec{m}^{\omega}(\vec{x})\right].\end{aligned} \tag{32}$$

Now, taking the cross product of Eq. (9) with $\vec{m}_G^{-\omega}$ and subtracting that of Eq. (19) [evaluated at $(-\omega)$] with $\vec{m}^{\omega}$, one obtains

$$\begin{aligned}&\nabla\phi^{\omega}(\vec{x})\cdot\vec{m}_G^{-\omega}(\vec{x}-\vec{x}')-\nabla\phi_G^{-\omega}(\vec{x}-\vec{x}')\cdot\vec{m}^{\omega}(\vec{x})\\ &=(D/M_s)\left[\vec{m}_G^{-\omega}(\vec{x}-\vec{x}')\cdot\nabla^2\vec{m}^{\omega}(\vec{x})-\vec{m}^{\omega}(\vec{x})\right.\\ &\left.\cdot\nabla^2\vec{m}_G^{-\omega}(\vec{x}-\vec{x}')\right].\end{aligned} \tag{33}$$

Using Eq. (33) in Eq. (32) and integrating by parts, one obtains the following extinction integral equation over the surfaces of the film:

$$0=\int_S d\vec{S}\cdot\left\{\phi^{\omega}(\vec{x})\vec{b}_G^{-\omega}(\vec{x}-\vec{x}')-\phi_G^{-\omega}(\vec{x}-\vec{x}')\vec{b}^{\omega}(\vec{x})-4\pi(D/M_s)\sum_{\tilde{j}}\left[m_{G\tilde{j}}^{-\omega}(\vec{x}-\vec{x}')\nabla m_{\tilde{j}}^{\omega}(\vec{x})-m_{\tilde{j}}^{\omega}(\vec{x})\nabla m_{G\tilde{j}}^{-\omega}(\vec{x}-\vec{x}')\right]\right\}. \tag{34}$$

In the case of a thin film, this previous extinction equation (34) corresponds to a convolution in the z and x directions in both surfaces of the sample; i.e., taking the Fourier transform of Eq. (34) in those directions, one transforms this integral equation into an algebraic equation for each independent value of the wave vector $\vec{Q}$ and frequency Ω:

$$\begin{aligned}0=&\phi(l)\left[b_y^G(l-y')-Q\phi^G(l-y')\right]-\phi(-l)\left[b_y^G(-l-y')+Q\phi^G(-l-y')\right]\\ &-\frac{d}{2}\left[\frac{\partial M_-}{\partial y}(l)M_+^G(l-y')+\frac{\partial M_+}{\partial y}(l)M_-^G(l-y')-\frac{\partial M_-}{\partial y}(-l)M_+^G(-l-y')-\frac{\partial M_+}{\partial y}(-l)M_-^G(-l-y')\right]\\ &+\frac{d}{2}\left[\frac{\partial M_-^G}{\partial y}(l-y')M_+(l)+\frac{\partial M_+^G}{\partial y}(l-y')M_-(l)-\frac{\partial M_-^G}{\partial y}(-l-y')M_+(-l)-\frac{\partial M_+^G}{\partial y}(-l-y')M_-(-l)\right],\end{aligned} \tag{35}$$

where we have used Eqs. (29), (30), and simplified notation by excluding labels $(\vec{Q},\omega)$ for the modes and $-(\vec{Q},\omega)$ for the Green's functions [again $M_{\pm}\equiv 4\pi(m_x\pm im_{\tilde{y}})$].

Using the form of Eqs. (24) for the solutions of the Green's functions in Fourier space in Eq. (35), one obtains the following set of extinction equations for the frequencies Ω of the modes of wave vector $\vec{Q}$. The following first set of three equations ($j=1,2,3$) arises for $y'<-l$:

$$\begin{aligned}0=&e^{-\alpha_j^u l}\left\{\left(\alpha_j^u-Q\right)A_j^u-(i/2)\cos\theta_M\left(B_{j+}^u-B_{j-}^u\right)\right\}\phi(l)-e^{\alpha_j^u l}\left\{\left(\alpha_j^u+Q\right)A_j^u-(i/2)\cos\theta_M\left(B_{j+}^u-B_{j-}^u\right)\right\}\phi(-l)\\ &-(d/2)e^{-\alpha_j^u l}\left\{\left[M_+'(l)+\alpha_j^u M_+(l)\right]B_{j-}^u+\left[M_-'(l)+\alpha_j^u M_-(l)\right]B_{j+}^u\right\}\\ &+(d/2)e^{\alpha_j^u l}\left\{\left[M_+'(-l)+\alpha_j^u M_+(-l)\right]B_{j-}^u+\left[M_-'(-l)+\alpha_j^u M_-(-l)\right]B_{j+}^u\right\},\end{aligned} \tag{36}$$

where $M_{\pm}'$ is shorthand for $\partial M_{\pm}/\partial y$, and the following set of three equations comes from the case $y'>l$:

$$\begin{aligned}0=&-e^{\alpha_j^d l}\left\{\left(\alpha_j^d+Q\right)A_j^d+(i/2)\cos\theta_M\left(B_{j+}^d-B_{j-}^d\right)\right\}\phi(l)+e^{-\alpha_j^d l}\left\{\left(\alpha_j^d-Q\right)A_j^d+(i/2)\cos\theta_M\left(B_{j+}^d-B_{j-}^d\right)\right\}\phi(-l)\\ &-(d/2)e^{\alpha_j^d l}\left\{\left[M_+'(l)-\alpha_j^d M_+(l)\right]B_{j-}^d+\left[M_-'(l)-\alpha_j^d M_-(l)\right]B_{j+}^d\right\}\\ &+(d/2)e^{-\alpha_j^d l}\left\{\left[M_+'(-l)-\alpha_j^d M_+(-l)\right]B_{j-}^d+\left[M_-'(-l)-\alpha_j^d M_-(-l)\right]B_{j+}^d\right\}.\end{aligned} \tag{37}$$

One way to solve these equations is to replace in them $B_{j\pm}^{u,d}$ in terms of $A_j^{u,d}$ using Eqs. (B8), (B9), (B12), and (B13), that follow since the Green's functions satisfy the Landau-Lifshitz equations, i.e.,

$$B_+^u=-iA^u(q+\alpha_u\cos\theta_M-ik\sin\theta_M)/\left[d\left(\alpha_u^2-Q^2\right)-h_i+\Omega\right]\equiv -iA^u b_+^u, \tag{38}$$

$$B_-^u=-iA^u(q-\alpha_u\cos\theta_M+ik\sin\theta_M)/\left[d\left(\alpha_u^2-Q^2\right)-h_i-\Omega\right]\equiv -iA^u b_-^u, \tag{39}$$

$$B_+^d = -iA^d(q - \alpha_d \cos\theta_M - ik\sin\theta_M)/\left[d\left(\alpha_d^2 - Q^2\right) - h_i + \Omega\right] \equiv -iA^d b_+^d, \tag{40}$$

$$B_-^d = -iA^d(q + \alpha_d \cos\theta_M + ik\sin\theta_M)/\left[d\left(\alpha_d^2 - Q^2\right) - h_i - \Omega\right] \equiv -iA^d b_-^d. \tag{41}$$

In this way, A^u and A^d cancel out in Eqs. (36) and (37), and defining $\tilde{M}_\pm \equiv -id M_\pm$, these equations become

$$\begin{aligned}
0 = {} & e^{-\alpha_j^u l}\left\{2\left(\alpha_j^u - Q\right) - \cos\theta_M\left(b_{j+}^u - b_{j-}^u\right)\right\}\phi(l) - e^{\alpha_j^u l}\left\{2\left(\alpha_j^u + Q\right) - \cos\theta_M\left(b_{j+}^u - b_{j-}^u\right)\right\}\phi(-l) \\
& - e^{-\alpha_j^u l}\left\{\left[\tilde{M}'_+(l) + \alpha_j^u \tilde{M}_+(l)\right]b_{j-}^u + \left[\tilde{M}'_-(l) + \alpha_j^u \tilde{M}_-(l)\right]b_{j+}^u\right\} \\
& + e^{\alpha_j^u l}\left\{\left[\tilde{M}'_+(-l) + \alpha_j^u \tilde{M}_+(-l)\right]b_{j-}^u + \left[\tilde{M}'_-(-l) + \alpha_j^u \tilde{M}_-(-l)\right]b_{j+}^u\right\},
\end{aligned} \tag{42}$$

$$\begin{aligned}
0 = {} & -e^{\alpha_j^d l}\left\{2\left(\alpha_j^d + Q\right) + \cos\theta_M\left(b_{j+}^d - b_{j-}^d\right)\right\}\phi(l) + e^{-\alpha_j^d l}\{2\left(\alpha_j^d - Q\right) + \cos\theta_M\left(b_{j+}^d - b_{j-}^d\right)\}\phi(-l) \\
& - e^{\alpha_j^d l}\left\{\left[\tilde{M}'_+(l) - \alpha_j^d \tilde{M}_+(l)\right]b_{j-}^d + \left[\tilde{M}'_-(l) - \alpha_j^d \tilde{M}_-(l)\right]b_{j+}^d\right\} \\
& + e^{-\alpha_j^d l}\left\{\left[\tilde{M}'_+(-l) - \alpha_j^d \tilde{M}_+(-l)\right]b_{j-}^d + \left[\tilde{M}'_-(-l) - \alpha_j^d \tilde{M}_-(-l)\right]b_{j+}^d\right\}.
\end{aligned} \tag{43}$$

In the previous six equations (42), (43) one should replace boundary conditions that relate $M'_\pm$ with $M_\pm$ on the surfaces of the film, and in this way one gets a consistent set of six homogeneous equations and six unknowns. In our case we use the boundary conditions of Eqs. (10) and (11) [23,26,27], which in terms of $M_\pm$ read

$$\frac{\partial M_\pm}{\partial n} = -\lambda \sin^2\theta_M M_\pm \pm \frac{\lambda}{2}\cos^2\theta_M (M_+ - M_-). \tag{44}$$

Notice that free boundary conditions, $\partial M_\pm/\partial n = 0$, correspond simply to the case $\lambda = 0$, i.e., no surface anisotropy. Replacing Eqs. (44) into the extinction equations (42), (43), these equations become effectively 6 equations for the 6 unknowns $\phi^\omega(\pm l)$, $M_\pm^\omega(\pm l)$:

$$\begin{aligned}
0 = {} & e^{-\alpha_j^u l}\left[2\left(\alpha_j^u - Q\right) - \cos\theta_M\left(b_{j+}^u - b_{j-}^u\right)\right]\phi(l) - e^{\alpha_j^u l}\left[2\left(\alpha_j^u + Q\right) - \cos\theta_M\left(b_{j+}^u - b_{j-}^u\right)\right]\phi(-l) \\
& + e^{-\alpha_j^u l}\left\{\left[\left(\lambda\sin^2\theta_M - \alpha_j^u\right)b_{j-}^u + (\lambda/2)\cos^2\theta_M\left(b_{j+}^u - b_{j-}^u\right)\right]\tilde{M}_+(l)\right. \\
& \left. + \left[\left(\lambda\sin^2\theta_M - \alpha_j^u\right)b_{j+}^u - (\lambda/2)\cos^2\theta_M\left(b_{j+}^u - b_{j-}^u\right)\right]\tilde{M}_-(l)\right\} \\
& + e^{\alpha_j^u l}\left\{\left[\left(\lambda\sin^2\theta_M + \alpha_j^u\right)b_{j-}^u + (\lambda/2)\cos^2\theta_M\left(b_{j+}^u - b_{j-}^u\right)\right]\tilde{M}_+(-l)\right. \\
& \left. + \left[\left(\lambda\sin^2\theta_M + \alpha_j^u\right)b_{j+}^u - (\lambda/2)\cos^2\theta_M\left(b_{j+}^u - b_{j-}^u\right)\right]\tilde{M}_-(-l)\right\},
\end{aligned} \tag{45}$$

$$\begin{aligned}
0 = {} & -e^{\alpha_j^d l}\left[2\left(\alpha_j^d + Q\right) + \cos\theta_M\left(b_{j+}^d - b_{j-}^d\right)\right]\phi(l) + e^{-\alpha_j^d l}\left[2\left(\alpha_j^d - Q\right) + \cos\theta_M\left(b_{j+}^d - b_{j-}^d\right)\right]\phi(-l) \\
& + e^{\alpha_j^d l}\left\{\left[\left(\lambda\sin^2\theta_M + \alpha_j^d\right)b_{j-}^d + (\lambda/2)\cos^2\theta_M\left(b_{j+}^d - b_{j-}^d\right)\right]\tilde{M}_+(l)\right. \\
& \left. + \left[\left(\lambda\sin^2\theta_M + \alpha_j^d\right)b_{j+}^d - (\lambda/2)\cos^2\theta_M\left(b_{j+}^d - b_{j-}^d\right)\right]\tilde{M}_-(l)\right\} \\
& + e^{-\alpha_j^d l}\left\{\left[\left(\lambda\sin^2\theta_M - \alpha_j^d\right)b_{j-}^d + (\lambda/2)\cos^2\theta_M\left(b_{j+}^d - b_{j-}^d\right)\right]\tilde{M}_+(-l)\right. \\
& \left. + \left[\left(\lambda\sin^2\theta_M - \alpha_j^d\right)b_{j+}^d - (\lambda/2)\cos^2\theta_M\left(b_{j+}^d - b_{j-}^d\right)\right]\tilde{M}_-(-l)\right\}.
\end{aligned} \tag{46}$$

The condition that the determinant associated with this 6×6 linear system of equations ($j = 1,2,3$) to be null determines the frequencies of the dipole-exchange modes of the thin film, and then the associated eigenvectors of this matrix may also be determined: they correspond to the modes evaluated at the surfaces of the film. Notice that the only unknown in the coefficients of this previous matrix is the frequency, and imposing the determinant to be zero effectively corresponds to a nonlinear equation for the frequency as a function of a given wave vector $\vec{Q}$. In practice one may obtain numerically the dispersion relation curves by doing contour plots at level zero, in the Ω-Q plane, of the imaginary and real parts of the determinant of Eqs. (45) and (46), something that is readily available in mathematical software, and that may be done very fast.

Thus, the main result of this work are Eqs. (42) and (43) since they allow one to determine the dispersion relation of the dipole-exchange modes of a thin film in a quite general configuration, i.e., with an applied magnetic field in an oblique direction and with boundary conditions of choice, which basically relate the normal derivative of the magnetization at the surfaces with the magnetization there. These boundary conditions may be different in both film surfaces and they may represent tensorial surface anisotropies or boundary conditions of more modern interest such as exchange bias [24] and the Dzyaloshinskii-Moriya interaction [25]. In the case of this work we illustrated the use of these equations by taking the partially pinned boundary conditions used in Ref. [19], which corresponds to uniaxial surface anisotropy of the same value in both film surfaces. Equations (45) and (46) follow by replacing in Eqs. (42) and (43) the just mentioned boundary conditions, i.e., Eqs. (44).

Our main focus is in ferromagnetic films surrounded by nonmagnetic media, in which case the electromagnetic boundary conditions of Eqs. (29) and (30) do apply. But, if one is interested in contact of the film with an ideal metallic

conductive layer, the boundary condition should be $b_y = 0$ in the corresponding surface, instead of the boundary conditions of Eqs. (29) and/or (30). The effect of this change in Eqs. (42)–(43), (45)–(46) is easily implemented: the terms proportional to Q in the first lines of these equations that accompany $\phi(l)$ and/or $\phi(-l)$ disappear if the respective conductive layer is at $y = l$ and/or $y = -l$.

Finally, Eqs. (45) and (46), or their analogs for other boundary conditions, allow one to determine the dipole-exchange spin-wave mode dispersion relations as well as their shapes at the surfaces of the film, and as explained in the following section this further allows one to determine the modes everywhere, if there is interest.

IV. DIPOLE-EXCHANGE MODES

The shape of the dipole-exchange spin-wave modes has been addressed in a number of works, but mostly in the context of standing-wave resonance (SWR) modes, or the $\vec{Q} \to 0$ limit. In these studies it became clear that the type of boundary condition that would apply determines the shapes of the modes close to the surfaces of the films. Not in the context of SWR, interesting studies of the shapes of dipole-exchange modes are those of Ref. [9], where the limit between microscopic and macroscopic dipole-exchange theories is explored, and those of Ref. [22], where in the context of a nonlinear study the effect of hybridization of modes on their shapes is investigated.

The present theory allows to determine in detail the dipole-exchange modes of the ferromagnetic film. In order to do this the basic tool is that Eq. (34) may be used whenever S represents a surface that surrounds a region of the sample that does not include a singularity of the Green's functions involved. Thus, if one is interested in determining the values of the modes at an interior position y' of the film, one chooses two regions $S^u_{y'}, S^d_{y'}$ surrounded by paths C_u, C_d as shown in Fig. 2, i.e., extending up to the upper and lower surfaces of the film and up to the surfaces just over and under y', respectively (the appropriate Green's functions that are used are the upper and lower Green's functions, as presented in the previous section). Also, in order to obtain the spin-wave modes in detail, these equations are written at the specific frequencies of the modes already obtained via the extinction equations, meaning additionally that one also knows the values of the modes on the surfaces of the film at those frequencies. This procedure leads to 6 equations for six unknowns, $\phi(y'), b_y(y'), (\partial M_\pm/\partial y)(y'), M_\pm(y')$; i.e., it allows one to determine completely the modes in the interior of the film. A similar procedure may be used in order to determine the modes in the exterior of the film. Details of this process of calculation of the dipole-exchange modes are presented in Appendix B2.

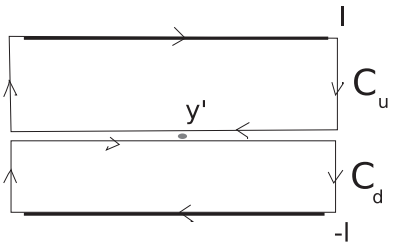

FIG. 2. Contours of integration for the determination of the dipole-exchange spin-wave modes at an interior position (y').

V. EXAMPLES OF DIPOLE-EXCHANGE DISPERSION CURVES IN FERROMAGNETIC FILMS

We proceed to plot several curves that represent dispersion curves of different dipole-exchange spin-wave modes for different parameters of the film, with some of the curves corresponding to comparisons with results of previous works. We stress the parameters that determine different dispersion curves: θ_H the angle of the applied magnetic field with respect to the plane of the film; φ the angle of the in-plane wave vector $\vec{Q}$ with respect to the direction of the applied field, i.e., $\vec{Q} = q\hat{x} + k\hat{z} = Q(\sin\varphi\hat{x} + \cos\varphi\hat{z})$; the scaled magnitude of the applied field $h \equiv H_0/4\pi M_s$; the scaled thickness of the film with respect to the exchange length $2l/l_{ex}$ ($l_{ex} = \sqrt{D/4\pi M_s}$); and the pinning parameter $\lambda = 2K_s/DM_s$. Also, the dispersion curves are described in terms of the scaled frequency $\Omega \equiv \omega/4\pi M_s|\gamma|$ and the scaled magnitude of the wave vector $|\vec{Q}|l_{ex}$ (in most cases that follow).

A. Films magnetized in-plane

In this section we consider films magnetized in-plane, i.e., $\theta_M = 0$. We consider first a Permalloy ferromagnetic film of thickness 360 nm, under an applied magnetic field in-plane $H_0 = (4\pi M_s)/5$ or $h = 0.2$, and with a pinning parameter $\lambda = 0.3$ (in this case the results for $\lambda = 0$ are quite similar). Figure 3 corresponds to the case $\varphi = 0$ or propagation parallel to the applied magnetic field, and Fig. 4 to $\varphi = \pi/2$ or perpendicular propagation.

This is a thick film since its thickness is 60 times the exchange length of Permalloy, $l_{ex} = 6$ nm, and the long-wavelength part of the lowest dipole-exchange dispersion

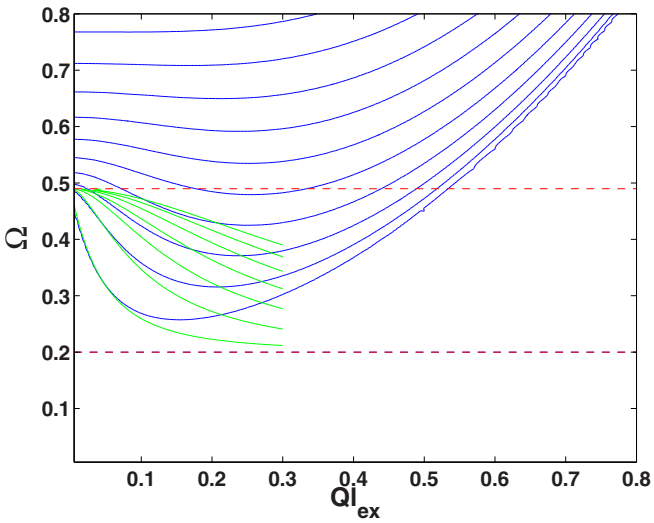

FIG. 3. Frequency dispersion relations of dipole-exchange (blue) and magnetostatic modes (green) of a Permalloy ferromagnetic film of thickness 360 nm, under an applied magnetic field in-plane $H_0 = 4\pi M_s/5$, and pinning parameter $\lambda = 0.3$ ($\Omega \equiv \omega/4\pi M_s|\gamma|$, and Q is the magnitude of the wave vector). Propagation parallel to the applied magnetic field ($\varphi = 0$).

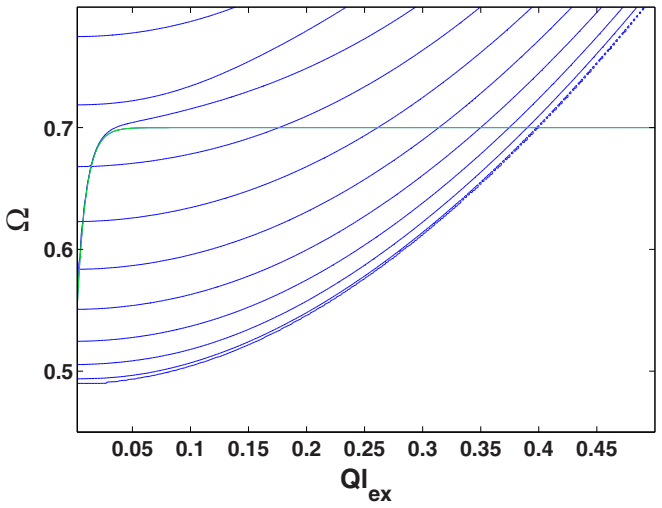

FIG. 4. Frequency dispersion relations of dipole-exchange (blue) and magnetostatic modes (green) of a Permalloy ferromagnetic film of thickness 360 nm, under an applied magnetic field in-plane. Parameters: $H_0 = 4\pi M_s/5$, pinning parameter $\lambda = 0.3$, $l_{ex} = 6$ nm ($\Omega \equiv \omega/4\pi M_s|\gamma|$, and Q is the magnitude of the wave vector). Propagation perpendicular to the applied magnetic field ($\varphi = \pi/2$).

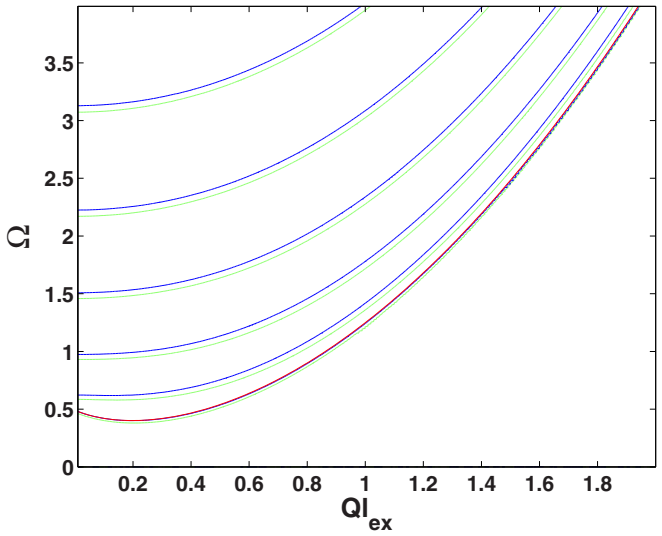

FIG. 5. Frequency dispersion relations of dipole-exchange modes of a thin ferromagnetic film of Permalloy of thickness 60 nm, under an applied magnetic field in-plane. Parameters: $H_0 = 4\pi M_s/5$, pinning parameters $\lambda = 0.3$ (green curves) and $\lambda = 0$ (blue curves), $l_{ex} = 6$ nm ($\Omega \equiv \omega/4\pi M_s|\gamma|$, and Q is the magnitude of the wave vector). The red curve corresponds to the very thin film approximation of Eq. (B28) for the frequency dispersion relation of the lowest dipole-exchange mode. Propagation parallel to the applied magnetic field ($\varphi = 0$).

curves (blue curves) should coincide with the corresponding dispersion curves of magnetostatic modes (green half-way curves), i.e., when the effect of the exchange interaction may be neglected. Indeed this is confirmed in these figures; the case $\varphi = 0$ of Fig. 3 corresponds to magnetostatic backward volume waves and the agreement with the lowest dipole-exchange modes is good up to $Ql_{ex} \simeq 0.1$, while in Fig. 4 for $\varphi = \pi/2$ the agreement is good up to $Ql_{ex} \simeq 0.02$, and the magnetostatic mode in this case corresponds to a Damon-Eshbach [1] forward surface mode (shown in green). Notice that we have plotted the frequency dispersion relations of magnetostatic modes using the results that we derive in Eqs. (B30) and (B31) via extinction equations, and these curves agree with those of Ref. [1]. Furthermore for $\varphi = 0$, i.e., propagation along the applied magnetic field in Fig. 3, we plotted the frequency limits of the backward volume magnetostatic modes with the dashed red curve [$\Omega = h$ and $\Omega = \sqrt{h(h+1)}$ respectively], and for $\varphi = \pi/2$ the Damon-Eshbach surface mode occurs in the frequency region between $\Omega = \sqrt{h(h+1)}$ and $\Omega = h + 1/2$ (the region of magnetostatic volume modes has shrunk to zero in this case; this topic is discussed in the next section).

In Fig. 5 we show dispersion relations for the case of a thin film of Permalloy magnetized in-plane, of thickness $2l = 60$ nm, i.e., ten times the exchange length, and for propagation parallel to the applied magnetic field, i.e., $\varphi = 0$. We plot dispersion curves for the cases $\lambda = 0$ (blue) and $\lambda = 0.3$ (green): it is seen that they go close together but with those corresponding to $\lambda = 0.3$ slightly lower. Also, since it is a thin film we plot the approximation for ultrathin films (red curve) of Eq. (B28), which coincides very well with the lowest mode corresponding to free boundary conditions or $\lambda = 0$.

A final example of in-plane magnetized films, with propagation perpendicular to the applied magnetic field ($\varphi = \pi/2$), corresponds to our Fig. 6 which can be compared with Fig. 1 of Ref. [8], which corresponds to an exact calculation using the PW approach, a comparison which is quite good. The curves correspond to a thick film of YIG, of thickness $2l = 610$ nm, with exchange length of 16.1 nm (i.e., $2l/l_{ex} \simeq 38$), an applied magnetic field equal to $2\pi M_s$, i.e., $h = 0.5$, and free boundary conditions ($\lambda = 0$).

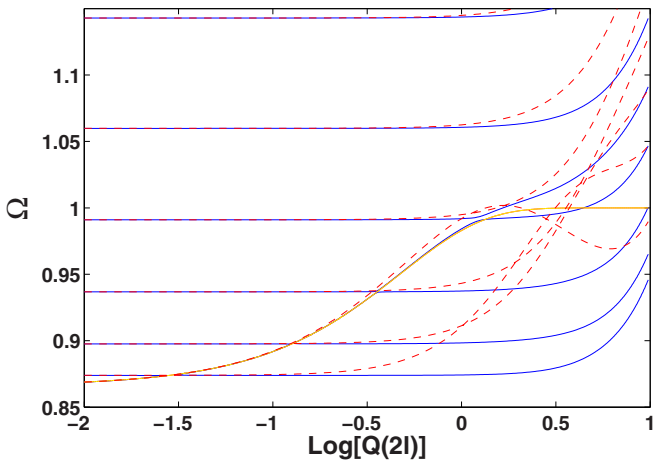

FIG. 6. Frequency dispersion relations of dipole-exchange modes of a ferromagnetic film of YIG of thickness $2l = 610$ nm, under an applied magnetic field in-plane. Parameters: $H_0 = 2\pi M_s$, pinning parameter $\lambda = 0$, $l_{ex} = 16.1$ nm ($\Omega \equiv \omega/4\pi M_s|\gamma|$, and Q is the magnitude of the wave vector). The yellow curve corresponds to the frequency dispersion of the magnetostatic Damon-Eshbach surface mode. Propagation perpendicular to the applied magnetic field ($\varphi = \pi/2$). The dashed red curves correspond to approximate dispersion relations proposed in Ref. [19].

As mentioned in that reference, the "rapidly rising curve" that hybridizes with exchange modes at crossover points has its origin in the magnetostatic Damon-Eshbach [1] surface mode (DE) that occurs in this geometry (the interpretation is that the volume modes that were degenerate in the magnetostatic approximation are up lifted by exchange and hybridize with the Damon-Eshbach mode, if they cross). We plotted the latter DE mode in yellow: it stays on top of the actual dipole-exchange mode up to the point of hybridization where the upper limit of the DE occurs (at $\Omega = h + 1/2$, which is equal to one in this case). In Fig. 6 we have also compared our results with the approximate dispersion relations of Ref. [19] [their Eqs. (45) and (46), and related]. The results of their formulas are given as dashed red curves, and the agreement in this case is not good; thus one should apply these approximate formulas with care.

B. Films magnetized perpendicularly to the plane

In this section we consider films magnetized perpendicularly to the plane, i.e., $\theta_M = \pi/2$. We consider here dispersion curves for a case of a film of YIG plotted in Ref. [19] in their Fig. 5(a), which in our case corresponds to Fig. 7. This is a thick film of 510 nm and the exchange length was considered as $l_{ex} = 17.6$ nm, i.e., $2l/l_{ex} \simeq 29$, $\varphi = 0$, or parallel propagation, and fully pinned boundary conditions (i.e., $\lambda \to \infty$; in our case we took $\lambda = 1000$). The agreement between our Fig. 7 and their Fig. 5(a) is relatively good, but in the case of free boundary conditions their Fig. 5(b) and our results have disagreements, especially in the crossover regions. In Fig. 7 we also plot the approximate dispersion relations proposed by Ref. [19] as red dashed curves [they follow from their Eqs. (45) and (46), and related]. These approximate dispersion curves were also plotted in Ref. [19], and we have agreement with those. The disagreement between the approximate dispersion curves and the exact ones may be attributed to repulsion between dispersion curves, an issue that is resolved in Ref. [19] through recourse to a perturbation theory.

Also, a simple configuration in which partially pinned boundary conditions may be tested corresponds to standing modes in perpendicularly magnetized films, with infinite wavelength in-plane, i.e., $Q = 0$. In Ref. [27] this case is discussed: frequencies are given by $\Omega = h_i + (k_y l_{ex})^2$, with k_y a wave vector perpendicular to the plane taking discrete values according to solutions to the equations $\cot(k_y l) = k_y/\lambda$ and $\tan(k_y l) = -k_y/\lambda$. We solved Eqs. (45) and (46) in the limit $Q \to 0$ for the frequencies of the standing modes in order to test these results (we used $Q l_{ex} = 0.001$): the agreement is perfect between our solutions and the solutions resulting from the equations cited in Ref. [27] and just presented.

C. Films magnetized obliquely

As examples, in the following we show plots of dispersion relations of dipole-exchange modes in the case of an obliquely applied magnetic field. We took Permalloy in the thin-film limit, with the same film parameters as those of Fig. 5, i.e., thickness $2l = 60$ nm, $l_{ex} = 6$ nm, pinning parameter $\lambda = 0.3$. The magnetic field is applied at an angle $\theta_H = \pi/4$ from the plane, and in order to compare with the results of Fig. 5, we adjusted the magnitude of H_0 so that $H_i \simeq 4\pi M_s/5$, i.e., $h_i \simeq 0.2$. These parameters lead through Eq. (1) to an inclination angle $\theta_M \simeq 0.166 \simeq \pi/20$ of the equilibrium magnetization from the plane. Figure 8 shows dispersion relations of dipole-exchange modes under the previous parameters, with the in-plane wave vector pointing in the direction of the projection of the applied magnetic field in the plane, i.e., $\varphi = 0$; in comparison with the in-plane case of Fig. 5 ($\varphi = 0$) the

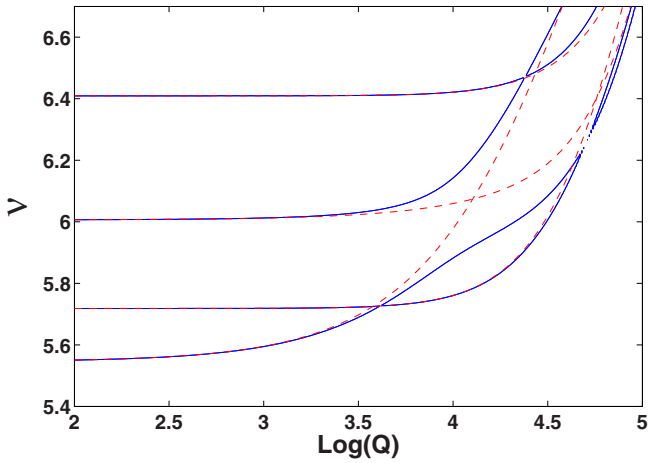

FIG. 7. Frequency dispersion relations of dipole-exchange modes of a ferromagnetic film of YIG of thickness 510 nm, under an applied magnetic field perpendicular to the plane. Parameters: $H_0 = 2.12(4\pi M_s)$, pinning parameter $\lambda = 1000$, $l_{ex} = 17.6$ nm, $\nu \equiv \omega/2\pi$ in units of GHz, and Q is the magnitude of the wave vector in units of cm^{-1}. The dashed red curves correspond to approximate dispersion relations proposed in Ref. [19].

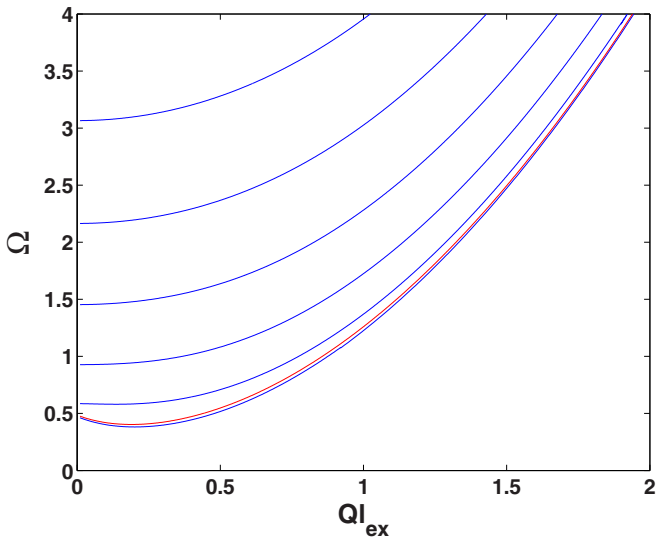

FIG. 8. Frequency dispersion relations of dipole-exchange modes of a thin ferromagnetic film of Permalloy of thickness 60 nm, under a magnetic field applied obliquely, $\theta_H = \pi/4$. Parameters: $H_i \simeq 4\pi M_s/5$, pinning parameter $\lambda = 0.3$, $l_{ex} = 6$ nm ($\Omega \equiv \omega/4\pi M_s|\gamma|$, and Q is the magnitude of the wave vector). The red curve corresponds to the very thin film approximation of Eq. (B28) for the frequency dispersion relation of the lowest dipole-exchange mode. Propagation parallel to the applied magnetic field ($\varphi = 0$).

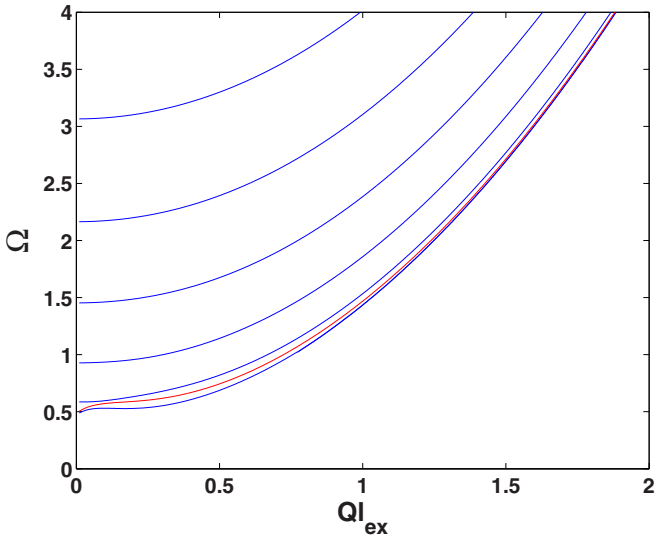

FIG. 9. Frequency dispersion relations of dipole-exchange modes of a thin ferromagnetic film of Permalloy of thickness 60 nm, under a magnetic field applied obliquely, $\theta_H = \pi/4$. Parameters: $H_i \simeq 4\pi M_s/5$, pinning parameter $\lambda = 0.3$, $l_{ex} = 6$ nm ($\Omega \equiv \omega/4\pi M_s|\gamma|$, and Q is the magnitude of the wave vector). The red curve corresponds to the very thin film approximation of Eq. (B28) for the frequency dispersion relation of the lowest dipole-exchange mode. Propagation at an angle $\varphi = \pi/4$ from the in-plane direction of the applied magnetic field.

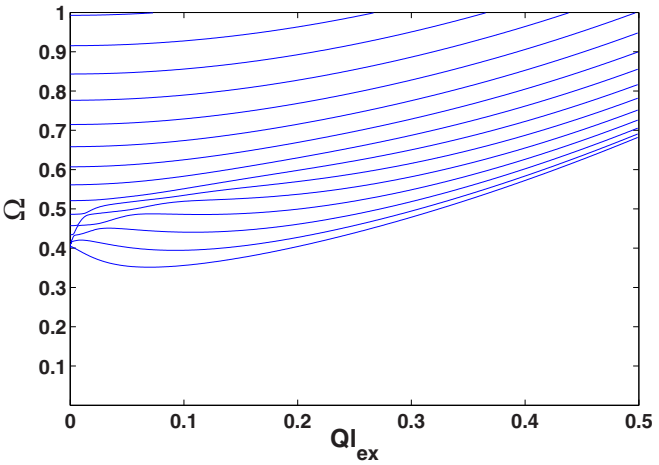

FIG. 10. Frequency dispersion relations of dipole-exchange modes of a ferromagnetic film of Permalloy of thickness 360 nm, under a magnetic field applied obliquely, $\theta_H = 7\pi/16$, $H_i \simeq 4\pi M_s/5$ or $h_i = 0.2$ ($\theta_M \simeq 0.7$), pinning parameter $\lambda = 0.3$, $l_{ex} = 6$ nm ($\Omega \equiv \omega/4\pi M_s|\gamma|$, and Q is the magnitude of the wave vector). Propagation at an angle $\varphi = \pi/4$ from the in-plane direction of the applied magnetic field.

structure of the dispersion curves is very similar, and one stills sees a minimum of the lowest dispersion curve at a nonzero wave vector, a feature of in-plane backward volume modes for angles of propagation φ close to the direction of the applied magnetic field. The red curve in Fig. 8 corresponds to the very thin film approximation of Eq. (B27) for the frequency dispersion relation of the lowest dipole-exchange mode, and it is seen to reproduce quite well the exact result in this case. Now in Eq. (B27) one sees explicitly the dependence on the angle θ_M of the dispersion relation for a given angle φ, and this explains the weak dependence of the frequency dispersion on θ_H in this case: indeed for $\theta_H = \pi/4$, $\theta_M \simeq \pi/20$, i.e., much smaller and close to $\theta_M = 0$ of Fig. 5.

Furthermore, Fig. 9 shows dispersion relations for the same previous parameters, but considering $\varphi = \pi/4$; in this case one sees that the dispersion relations are very similar to the case $\varphi = 0$ of Fig. 8, except for the lowest mode that flattens out showing the same feature that happens at lower θ_H, i.e., that as φ increases the minimum of the dispersion relation at a finite wave vector disappears. Again, the red curve on Fig. 9 corresponds to the very thin film approximation of Eq. (B27) for the frequency dispersion relation of the lowest dipole-exchange mode: it is seen to reproduce quite well the lowest mode for higher wave vectors, while staying between both lowest modes at low wave vectors.

From these results, without doing an extensive study of dispersion relations under oblique applied fields, one may expect mainly a continuous evolution of the dispersion relations from their shapes in the magnetized in-plane case to the perpendicularly magnetized one, with higher changes expected as θ_M grows faster at higher values of θ_H. The latter comment is justified by the results presented in Fig. 10 with dispersion relations of dipole-exchange modes that correspond to Permalloy, with $l_{ex} = 6$ nm, $\lambda = 0.3$, and a magnetic field applied at an angle $\theta_H = 7\pi/16 \simeq 1.37$, $h = 0.79$ so that $h_i = 0.2$ ($\theta_M \simeq 0.7$), $\varphi = \pi/4$; i.e., they do correspond to the parameters of the magnetostatic case of Fig. 15: particularly one sees that the lowest dispersion curves of the dipole-exchange modes resemble in the limit $Q \ll 1$ the magnetostatic modes of Fig. 15; i.e., they would coalesce at $\sqrt{h_i^2 + h_i \cos^2\theta_M}$ at $Q = 0$.

VI. EXAMPLES OF DIPOLE-EXCHANGE SPIN-WAVE MODES

In Secs. IV and B 2 it is explained how to determine the shapes of the spin-wave modes inside or outside the sample, once their frequencies for a given wave vector were determined by solving the eigenvalue problem of Eqs. (45) and (46). As examples of this procedure in the following we plot some dipole-exchange spin-wave modes for specific parameters.

We consider Permalloy magnetized in-plane by a magnetic field $H_0 = 4\pi M_s/5$, with exchange length $l_{ex} = 6$ nm, thickness $2l = 26.2$ nm, $\varphi = 0$, and pinning parameter $\lambda = 0.3$. The boundary condition Eqs. (10) and (11) in this in-plane case read $\partial m_y/\partial n = -\lambda m_y$ and $\partial m_x/\partial n = 0$; i.e., the in-plane m_x component is effectively free. We consider the mode with the lowest frequency ($\Omega = \omega/4\pi M_s|\gamma| = 0.68$), with in-plane wave vector chosen such that $Ql_{ex} = 0.628$: it has a quasiuniform shape across the thickness. Figure 11 reflects this: it shows the m_x and m_y components of this particular mode as a function of the thickness dimension y/l_{ex}; only the m_y component shows perturbations close to the surfaces and finite slopes there due to partial pinning (notice that the plots correspond to a specific time or phase).

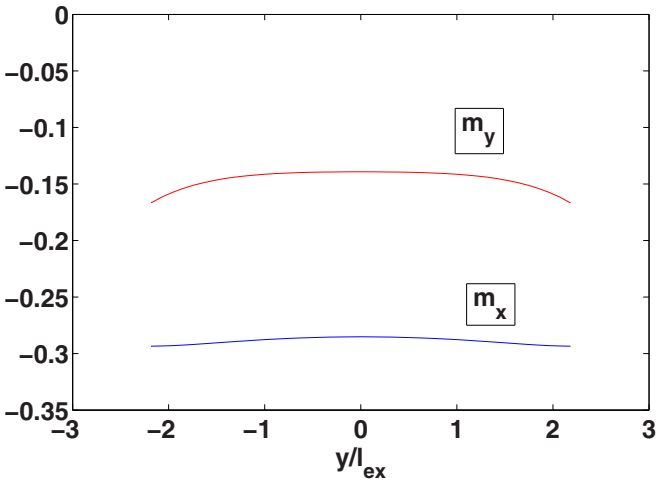

FIG. 11. Magnetization components $m_{x,y}$ along the thickness of the film of the lowest dipole-exchange mode of a Permalloy ferromagnetic film magnetized in-plane. Parameters are applied magnetic field $H_0 = 4\pi M_s/5$, thickness $2l = 26.2$ nm, $l_{ex} = 6$ nm, pinning parameter $\lambda = 0.3$, $\varphi = 0$, and $Ql_{ex} = 0.628$ ($\Omega = \omega/4\pi M_s|\gamma| = 0.68$). The mode is plotted at a particular time or phase.

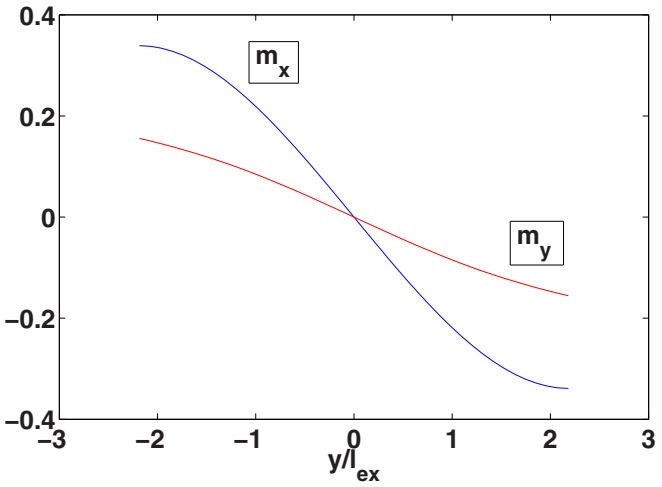

FIG. 12. Magnetization components $m_{x,y}$ along the thickness of the film of the second dipole-exchange mode of a Permalloy ferromagnetic film magnetized in-plane. Parameters are applied magnetic field $H_0 = 4\pi M_s/5$, thickness $2l = 26.2$ nm, $l_{ex} = 6$ nm, pinning parameter $\lambda = 0.3$, $\varphi = 0$, and $Ql_{ex} = 0.001$ ($\Omega = \omega/4\pi M_s|\gamma| = 1.00$). The mode is plotted at a particular time or phase.

Furthermore, Fig. 12 plots $m_{x,y}$ for a mode with the same parameters as before, except that it corresponds to a very long wavelength in-plane ($Ql_{ex} = 0.001$) and to the second mode in terms of increasing frequency ($\Omega = \omega/4\pi M_s|\gamma| = 1.01$); i.e., it is a standing mode along the thickness. In this figure one clearly sees one node; again the m_x component has zero slope on the surfaces as expected, and the m_y component has finite slope on the surfaces as a result of the pinning condition (an effective wavelength along the y direction becomes longer). Analogous results for $\lambda = 0$, i.e., for free boundary conditions, are not plotted, but they correspond to slightly higher frequencies in comparison with the $\lambda = 0.3$ case.

VII. DISCUSSION OF SOLUTIONS

As already mentioned Eqs. (42) and (43) are the main result of this work, since they allow one to determine the frequencies and eigenvectors at the surfaces of the dipole-exchange modes once appropriate boundary conditions have been replaced in them. Equations (45) and (46) result replacing in the previous equations the boundary conditions of partial pinning of Eq. (44), which correspond to uniaxial surface anisotropy of the same character in both surfaces of the film [19]. Here we discuss how to understand solutions to this homogeneous system of 6×6 matrix eigenvalue equations [Eqs. (45), (46)], in particular the frequency dispersion relations that follow from them as well as expected effective wavelengths along the direction perpendicular to the plane of the film.

The focus of the discussion will be on the fact that most of the different curves of frequency dispersions appear in ranges of frequencies where the parameters $\alpha^{(u,d)}$ do have purely imaginary solutions, or correspond to effective perpendicular real wave vectors. The latter parameters $\alpha^{(u,d)}$ appear in Eqs. (24) for the Fourier components of the interior Green's functions, and they do satisfy Eqs. (25), i.e., equations for the zeros of sixth-order polynomials. Notice that if one looked for plane-wave-type solutions (proportional to $\exp[-i(qx + \kappa_y y + kz - \Omega t')]$) to the dynamic equations for the linear modes, i.e., Eqs. (6) and (9), one would get basically Eqs. (25) for the relation between the wave vectors and the frequency, but with $\alpha^u = i\kappa_y$, or $\kappa_y^2 = -\alpha_u^2$. Thus, one may regard the extinction equations for the modes (45) and (46) as a set of convolution equations imposing the boundary conditions on a set of plane-wave solutions, which will have solutions at specific frequencies, with corresponding associated specific $\kappa_y(\Omega)$ wave vectors (complex or not, and six of them). Note that although our treatment is in terms of Green's functions, the use of straightforward pure plane-wave-type solutions instead of Green's functions is possible since the requirement for the validity of the extinction equations is to use solutions to the equations of motion in the convolutions: in this way equations for the modes are obtained.

We start discussing the solution to the magnetostatic extinction equations (B30), (B31), which is a simpler case to analyze, and which guides the understanding of the more complex dipole-exchange equations (45), (46). In this case the equation for α_u (B36) has as solutions $\alpha_u = Q\tilde{\alpha}_u$, with $\tilde{\alpha}_u$ satisfying the following equation ($k = Q\cos\varphi$, $q = Q\sin\varphi$):

$$0 = \left(h_i^2 + h_i\cos^2\theta_M - \Omega^2\right)\tilde{\alpha}_u^2 - 2ih_i\cos\varphi\sin\theta_M\cos\theta_M\tilde{\alpha}_u + \Omega^2 - h_i^2 - h_i(1 - \cos^2\varphi\cos^2\theta_M), \tag{47}$$

which leads to solutions

$$\tilde{\alpha}_u = \frac{\alpha_u}{Q} = \frac{ih_i\cos\varphi\sin\theta_M\cos\theta_M \pm \sqrt{\left(\Omega^2 - h_i^2 - h_i\right)\left(\Omega^2 - h_i^2 - h_i\sin^2\varphi\cos^2\theta_M\right)}}{h_i^2 + h_i\cos^2\theta_M - \Omega^2}, \tag{48}$$

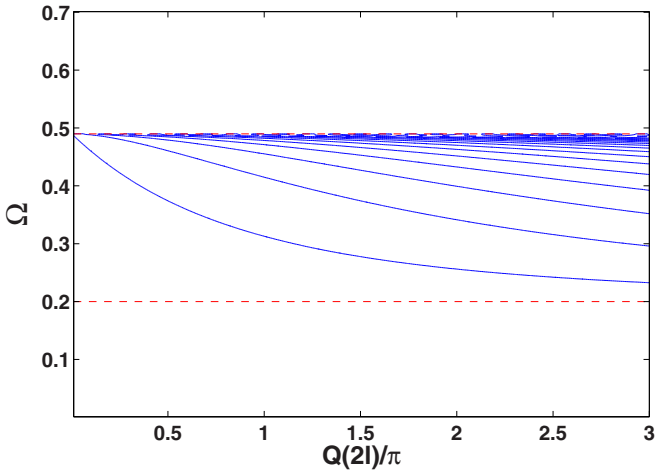

FIG. 13. Magnetostatic dispersion relations of a ferromagnetic thin film magnetized in-plane, propagation along the direction of the applied magnetic field ($\varphi = 0$). Dashed red lines represent the limiting frequencies of the volume modes in this case, i.e., $\Omega = h_i$ and $\Omega = \sqrt{h_i(h_i+1)}$, with $h = h_i = 0.2$.

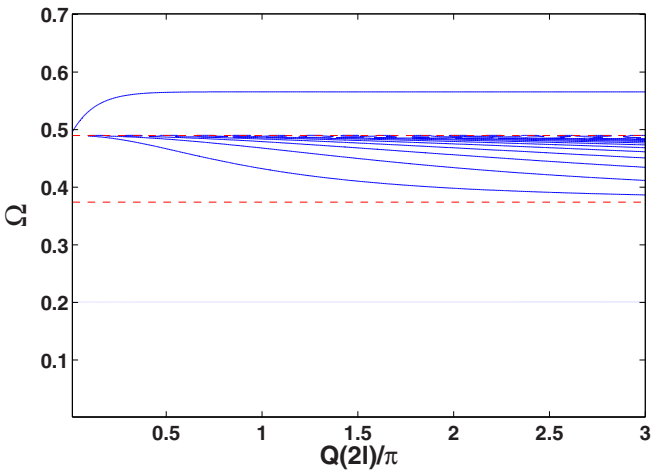

FIG. 14. Magnetostatic dispersion relations of a ferromagnetic thin film magnetized in-plane, propagation along the direction $\varphi = \pi/4$ of the applied magnetic field. Dashed red lines represent the limiting frequencies of the volume modes in this case, i.e., $\Omega = \sqrt{h_i^2 + h_i \sin^2\varphi}$ and $\Omega = \sqrt{h_i(h_i+1)}$, with $h = h_i = 0.2$. The mode of highest frequency is a Damon-Eshbach surface mode.

and the negatives of these solutions for $\tilde{\alpha}_d$. A well-studied geometry corresponds to the in-plane case $\theta_M = 0$, by Damon and Eshbach in Ref. [1], where the solution to the previous equation leads to

$$\alpha_u^2 = Q^2\left(h_i^2 + h_i \sin^2\varphi - \Omega^2\right)\Big/\left(h_i^2 + h_i - \Omega^2\right), \qquad (49)$$

with $h_i = h$ in this in-plane case. Thus for propagation parallel to the magnetization ($\varphi = 0$) $\alpha_u^2 = Q^2/\mu$ with $\mu \equiv (h_i^2 + h_i - \Omega^2)/(h_i^2 - \Omega^2)$, or $\alpha_u^2 < 0$ for $h_i < \Omega < \sqrt{h_i(h_i+1)}$; i.e., α_u is purely imaginary in this interval or there are effective perpendicular wave vectors along the perpendicular direction to the plane of the film. This is consistent with Ref. [28] which predicts oscillatory solutions for magnetostatic modes in regions where locally $\mu < 0$, which corresponds to a region where the underlying differential equation for the magnetostatic potential is hyperbolic. Furthermore, if φ is finite with magnetization still in-plane, $\alpha_u^2 < 0$ for $\sqrt{h_i^2 + h_i \sin^2\varphi} < \Omega < \sqrt{h_i(h_i+1)}$; i.e., this interval shrinks, although it is still within the region with $\mu < 0$. The number of oscillatory solutions along the direction perpendicular to the plane in these intervals and the fact that the interval shrinks as φ grows can be seen comparing Fig. 13 ($\varphi = 0$) and Fig. 14 ($\varphi = \pi/4$) for this case of in-plane magnetization ($h = h_i$ was chosen as 0.2). In Fig. 14 one also sees the well-known surface Damon-Eshbach mode that appears at $\varphi > \arctan(\sqrt{h})$ [1], with frequency greater than $\sqrt{h(h+1)}$, and with α real. In both previous figures the mentioned interval of frequencies with these oscillatory solutions is delimited within the red dashed curves; i.e., the results are consistent since except for the surface mode all the dispersion curves lie in this interval.

For the case of magnetic field applied obliquely, the expression of Eq. (48) shows that there are values of α that are purely imaginary in the interval of frequencies $\sqrt{h_i^2 + h_i \sin^2\varphi \cos^2\theta_M} < \Omega < \sqrt{h_i(h_i+1)}$. Figure 15 exemplifies this: θ_H was taken as $7\pi/16$; i.e., close to $\pi/2$ or the perpendicular case, the magnitude of the applied field was adjusted so that $h_i = 0.2$ ($h \simeq 0.79$), and φ was chosen as $\pi/4$. Most of the modes in this latter figure lie as predicted within the previously mentioned interval, and there is one mode that leaves this interval at a particular wave vector and becomes a surface mode with an oscillatory part (complex wave vector), this shows how the Damon-Eshbach surface mode of the in-plane case evolves. We also include Fig. 16 which corresponds to the perpendicular case ($\theta_M = \pi/2$): in this case the modes lie in the interval $h_i < \Omega < \sqrt{h_i(h_i+1)}$, a surface mode does not exist anymore (as insinuated by the evolution from Fig. 14 to Fig. 15), and one sees that

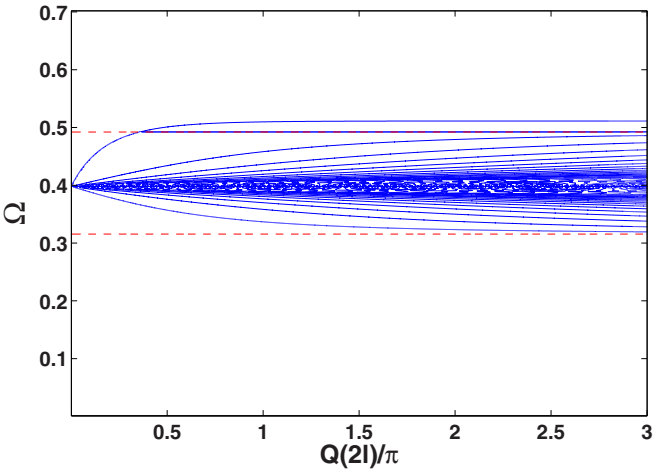

FIG. 15. Magnetostatic dispersion relations of a ferromagnetic thin film under an applied magnetic field at an angle $\theta_H = 7\pi/16$, propagation along the direction $\varphi = \pi/4$ of the applied magnetic field. Dashed red lines represent the limiting frequencies of the volume modes in this case, i.e., $\Omega = \sqrt{h_i^2 + h_i \sin^2\varphi \cos^2\theta_M}$ and $\Omega = \sqrt{h_i(h_i+1)}$, with $h_i = 0.2$. The mode of highest frequency is a surface mode with oscillatory character over a certain in-plane wave vector Q.

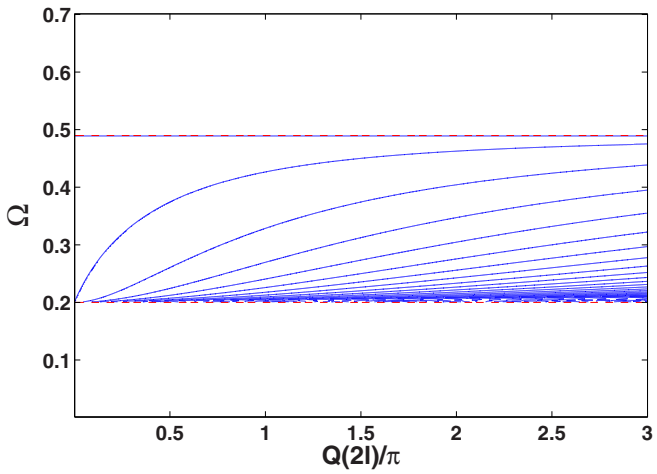

FIG. 16. Magnetostatic dispersion relations of a ferromagnetic thin film magnetized perpendicularly to the plane. Dashed red lines represent the limiting frequencies of the volume modes in this case, i.e., $\Omega = h_i$ and $\Omega = \sqrt{h_i(h_i+1)}$, with $h_i = 0.2$.

the dispersion curves of Fig. 15 represent an intermediate configuration between Figs. 13 and 16. Also notice that if one looks for the solutions of the magnetostatic equations for the modes Eqs. (B30), (B31), in the limit $Q \to 0$, the dispersion curves coalesce at $\Omega = \sqrt{h_i^2 + h_i \cos^2\theta_M}$, which is consistent with all the previous figures, in particular with Fig. 15. According to Eq. (48) this latter frequency corresponds to $\alpha \to \infty$ as the denominator goes to zero at this frequency.

Furthermore, from the structure of the magnetostatic extinction equations (B30), (B31) one may explain why there are several solutions when the α's are purely imaginary. This would happen since the elements of the associated matrix have as factors exponentials of the form $\exp(\pm\alpha l)$ that become harmonic oscillatory functions as the α's become purely imaginary solutions of the quadratic equations for the α's [Eqs. (B36), (B37)]: one may expect different solutions every time the arguments αl change by $i\pi/2$ as a result of α being a function of frequency for these particular two imaginary roots.

Now we discuss the solutions of the dipole-exchange modes that follow from Eqs. (45), (46). First, we analyze the limit $Q \to 0$. The α's are the roots of the sixth-order polynomial of Eq. (25), and in the limit $Q \to 0$ there are two solutions $\alpha = 0$, and the other four solutions satisfy ($\gamma \equiv h_i - d\alpha^2$):

$$\gamma^2 + \cos^2\theta_M \gamma - \Omega^2 = 0, \tag{50}$$

with both α_u and α_d satisfying the same equation. Thus, we have as solutions

$$\begin{aligned}\gamma_\pm &= -\cos^2\theta_M/2 \pm \sqrt{(\cos^2\theta_M/2)^2 + \Omega^2} \to d\alpha_\pm^2 \\ &= h_i + \cos^2\theta_M/2 \mp \sqrt{(\cos^2\theta_M/2)^2 + \Omega^2}.\end{aligned} \tag{51}$$

Thus, there are four solutions $\alpha_+^\pm$,$\alpha_-^\pm$ with origin in the exchange interaction; i.e., if $d = 0$ they do not exist (they go to infinity). The roots $\alpha_-^\pm$ are always real:

$$\alpha_-^\pm = \pm\sqrt{h_i + \cos^2\theta_M/2 + \sqrt{(\cos^2\theta_M/2)^2 + \Omega^2}}. \tag{52}$$

The roots $\alpha_+^\pm$ are real or purely imaginary depending on the frequency; the crossover frequency is $\Omega_L = \sqrt{h_i^2 + h_i\cos^2\theta_M}$ (where $\alpha_+^\pm = 0$):

$$\begin{aligned}\alpha_+^\pm &= \pm\sqrt{h_i + \cos^2\theta_M/2 - \sqrt{(\cos^2\theta_M/2)^2 + \Omega^2}} \to \Omega < \Omega_L, \\ \alpha_+^\pm &= \pm i\sqrt{-h_i - \cos^2\theta_M/2 + \sqrt{(\cos^2\theta_M/2)^2 + \Omega^2}} \to \Omega > \Omega_L.\end{aligned} \tag{53}$$

In the limit $Q \to 0$ the 6×6 homogeneous system of extinction dipole-exchange equations (45), (46) reduces to the following simpler 4×4 system (γ taking the values $\gamma_\pm$ leads to the four required equations):

$$\begin{aligned}0 = {} & e^{-\alpha_u l}\{[(\alpha_u - \lambda\sin^2\theta_M)(\Omega-\gamma) - \gamma\lambda\cos^2\theta_M]\tilde{M}_+(l) \\ & + [(\alpha_u - \lambda\sin^2\theta_M)(\Omega+\gamma) + \gamma\lambda\cos^2\theta_M]\tilde{M}_-(l)\} \\ & - e^{\alpha_u l}\{[(\alpha_u + \lambda\sin^2\theta_M)(\Omega-\gamma) + \gamma\lambda\cos^2\theta_M]\tilde{M}_+(-l) \\ & + [(\alpha_u + \lambda\sin^2\theta_M)(\Omega+\gamma) - \gamma\lambda\cos^2\theta_M]\tilde{M}_-(-l)\},\end{aligned} \tag{54}$$

with an analogous set of two equations replacing α_u by $-\alpha_d$. The numerical solutions to these equations correspond to the standing modes (SWR, or $\vec{Q} \to 0$), and were verified to give the right limit of the dipole-exchange dispersion relations of the numerical examples presented in the previous section. These limits do not depend on φ, as expected due to continuity, and they allow one to quantify the number of dipole-exchange dispersion relations (which evolve as Q grows from these points for different values of φ, at a given value of θ_M). As argued previously, solutions to this system of equations coincide with the range where the $\alpha_+^\pm$ are purely imaginary, i.e., when $\Omega > \Omega_L = \sqrt{h_i^2 + h_i\cos^2\theta_M}$: the different solutions may be associated with effective wave vectors perpendicular to the plane of the film, $k_y = \pm|\alpha_+|$, evaluated at the particular frequency of the eigenmode.

We now turn to a discussion of the solution of the extinction equations (45), (46) when $Q \neq 0$. The α's that appear in these equations are 6 solutions to the sixth-order polynomial equations in α_u,α_d, Eqs. (25) (the 6 solutions for the α_d are the negatives of those for the α_u, and three of those six solutions are chosen for α_u and α_d, respectively). One interesting point to mention is that in the general case of an obliquely applied magnetic field we have found numerically that a pair of purely imaginary solutions for the α's exist in a range of frequencies, for a given $Q \neq 0$. These solutions for α's are the continuation of the purely imaginary solutions at $Q = 0$ just presented, and correspond to the ranges of frequencies where the extinction equations (45), (46) have most of the eigensolutions. The fact

that one sees pairs of purely imaginary solutions for α's to Eqs. (25) in a range of frequencies may be explained since if one replaces in these equations $\alpha_u = iK_y$, i.e., as purely imaginary with K_y real, one may solve for Ω^2 as

$$\Omega^2 = \Omega_K^2 + \Omega_K \frac{[(\vec{K} \times \hat{\vec{z}})_x]^2 + K_x^2}{K^2} = \Omega_K^2 + \Omega_K \frac{(K_y \cos\theta_M - Q\cos\varphi \sin\theta_M)^2 + Q^2 \sin^2\varphi}{K_y^2 + Q^2}, \tag{55}$$

where $\vec{K}$ has been defined as $\vec{K} = K_x\hat{x} + K_y\hat{y} + K_z\hat{z}$, $q = K_x = Q\sin\varphi$, $k = K_z = Q\cos\varphi$, $\vec{Q} = k_x\hat{x} + k_z\hat{z}$ in the previous notation, and $\Omega_K \equiv h_i + dK^2$ ($\hat{\vec{z}}$ is the direction of the equilibrium magnetization). This explicit expression for Ω in terms of the wave vector $\vec{K}$ means that given $\vec{Q}$ there are real frequencies Ω associated with real wave vectors K_y. The question then is which of these values of K_y may represent eigenmodes: this is answered by solving the extinction equations (45), (46) which include other complex wave vectors that effectively allow one to solve the boundary conditions at specific frequencies. Similarly to the magnetostatic case, the extinction equations (45), (46) have a pair of equations with coefficients proportional to $\exp(\pm iK_y l)$, i.e., of oscillatory character, which would explain why there are several solutions as K_y changes as a function of Ω for fixed $\vec{Q}$. With respect to the latter one may be more quantitative: the 6×6 determinant that follows from Eqs. (45), (46) and that is zero at the eigenfrequencies is proportional to these oscillating terms of the type $\exp(\pm iK_y l)$ since these factors appear in all coefficients of two rows of this determinant (in these two rows one has these two real wave vectors associated with volume modes), and it is known that a determinant is proportional to the coefficients of any row or any column. Indeed, one may expect one new solution every time $K_y l$ changes by $\pi/2$. But notice that the analysis is not so straightforward for the case of an obliquely applied magnetic field. In the simpler cases of in-plane or perpendicular magnetization the relation of Eq. (55) between the frequency Ω and K_y depends on K_y^2, meaning that $\pm K_y$ lead to the same frequency, but in the oblique case for a given Ω one has corresponding positive and negative values of K_y of different absolute value: this means that an oscillatory eigenmode of a given frequency will have contributions from positive and negative wave vectors along the perpendicular direction of differing absolute values. In the simpler case of magnetization in-plane in Fig. 17 we exemplify how Eq. (55) explains qualitatively the appearance of the actual dispersion relations: we chose the parameters of Fig. 3, and we plotted the curves that follow from Eq. (55) assuming that the wave vectors take the form $K_y = \pi n/2l$, with n an integer, or equivalently effective wavelengths $\lambda_n = 2\pi/K_y = 2(2l)/n$. In this in-plane case Eq. (55) takes the form $\Omega^2 = \Omega_K^2 + \Omega_K(K_y^2 + Q^2\sin^2\varphi)/(K_y^2 + Q^2)$. The dashed red curves of Fig. 17 correspond to plotting the previous explicit expression for $\Omega(Q, K_y = \pi n/2l)$: one sees a close agreement with the actual dispersion relations; i.e., they explain qualitatively (and quantitatively in some ranges) the dispersion relations of the dipole-exchange spin-wave modes in this case.

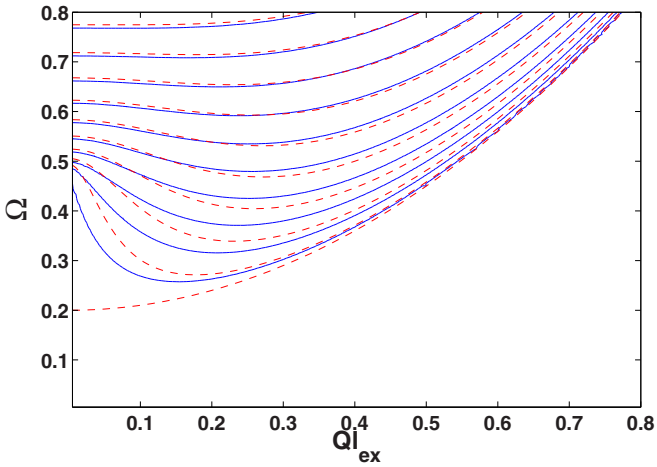

FIG. 17. Frequency dispersion relations of dipole-exchange (blue) of a Permalloy ferromagnetic film of thickness 360 nm, under an applied magnetic field in-plane $H_0 = 4\pi M_s/5$, pinning parameter $\lambda = 0.3$ ($\Omega \equiv \omega/4\pi M_s|\gamma|$, and Q is the magnitude of the wave vector), and propagation parallel to the applied magnetic field ($\varphi = 0$). Comparison is made with frequencies associated with perpendicular wave vectors $K_y = \pi n/2l$ from Eq. (55), with n an integer: dashed red curves (n grows from zero at the lowest dashed curve).

VIII. DISCUSSION OF EXPERIMENTAL RESULTS

In the following we discuss the relation between the presented theoretical results on dipole-exchange spin-wave modes of ferromagnetic films and a selection of experimental results that have been published on the subject. Experimental results on spin-wave modes of ferromagnetic films may be broadly classified as those associated with microwave spectroscopy and light spectroscopy. With respect to microwave spectroscopy one may distinguish studies on traditional ferromagnetic resonance (FMR) using microwave cavities that are mainly associated with detection of standing spin-wave modes (SWR), and studies in propagating spin-wave spectroscopy (PSW) that rely on exciting and detecting spin waves through proper antennas (also parametric excitation has been used to study dipole-exchange spin waves in thin films in a nonlinear regime). Brillouin light scattering (BLS) has been the main technique in order to study spin waves in ferromagnetic films using light.

With respect to traditional FMR, which uses a resonant cavity operating at a specified microwave frequency, it basically excites modes of very long in-plane wavelength ($\vec{Q} = 0$), and is associated with the excitation of standing spin-wave modes with spatial variation in the direction perpendicular to the plane of the film, i.e., standing-wave resonance (SWR) (it is mainly the exchange interaction that contributes to the frequencies of these standing modes). In 1958 Seavey and Tannenwald [29], following Kittel's prediction [30] that under pinning conditions odd standing spin-wave modes should be seen in FMR, did find experimental evidence consistent with this prediction in a Permalloy film of 560 nm thickness (the even modes were slightly seen in principle due to a gradient in the magnetic field). In particular we tested our theoretical

model with respect to SWR results, by comparing the results of our Eqs. (54), which apply for dipole-exchange modes in the limit $\vec{Q} \to 0$, to the experimental results of Lykken [31] on "flash-evaporated" Permalloy. This sample was a high-quality sample magnetized perpendicularly to the plane: we get very good agreement with the experimental frequencies of the standing modes by using fully pinned boundary conditions in both surfaces and their parameters for this Permalloy film, i.e., $l_{ex} = 4.23$ nm, thickness $2l = 220$ nm, $4\pi M_s = 10.6$ kOe, and cavity frequency $\nu = 12.33$ GHz. Studies on standing waves have been reviewed by Frait [32], Weber [33], Puszkarski [34,35], Wigen *et al.* [36], and others. Explanations for the experimental results include partial pinning models (with eventually different properties in both surfaces of the films), dynamic pinning models, inhomogeneities in the interior, tensorial surface anisotropy, etc. With the model presented in this work issues such as partial pinning and tensorial surface anisotropies can be addressed in order to compare with experiments, even if both surfaces behave differently: one needs to replace the boundary conditions that would represent these more general conditions in both surfaces in Eqs. (42), (43) and then proceed to obtain a simpler system at $\vec{Q} \to 0$, as was done in Eqs. (54) for boundary conditions of partial pinning that are equivalent on both surfaces of the film.

In 1994 Kalinikos [4] did a comparison of his theory with Slavin on dipole-exchange modes [19] with several experimental works on microwave spectroscopy in ferromagnetic films mainly dealing with propagating spin-wave modes, launched and detected by microstrip antennas. The agreement between theory and experiment is good, and there is also a discussion of the effect of pinning conditions at the surfaces. Notice that the theoretical results presented in this work agree with those of Kalinikos and Slavin [19] in its full version, which involves the diagonalization of large matrices. Recently Maksymov and Kostylev [37] have reviewed the topic of broadband stripline ferromagnetic resonance spectroscopy from a more modern perspective in ferromagnetic films, multilayers, and nanostructures.

There is also a particular work [38] where the interaction of optical waveguide modes with dipole-exchange surface spin waves in a $Lu_{2.14}Bi_{0.86}Fe_{4.94}Mg_{0.06}O_{12}$ ferrimagnetic film was studied: spin waves were launched and detected by gold wire antennas and parallel optical waveguide modes were also excited in the film. They plotted experimental results of a dipole-exchange spin wave spectrum that shows that the Damon-Eshbach surface mode of dipolar origin hybridizes with the standing modes of exchange origin and they compare with theory (the film is magnetized in-plane and the spin-wave propagation is perpendicular to the direction of the in-plane applied magnetic field). We compared their results with our theory too: we find very good agreement with their Fig. 2 if we take the magnitude of the applied magnetic field as $0.623(4\pi M_s)$, a value that was not given in the paper (following their text, we took other parameters as belonging to a film of YIG of thickness 4.5 μm, $4\pi M_s = 1\,800$ Oe, $l_{ex} = 17.6$ nm).

With respect to Brillouin light scattering, this is an experimental technique that allows one to study spin-wave modes of finite wave vectors. In 1994 Dutcher [39] presented a comparison of experimental results on BLS of spin-wave modes in ferromagnetic films with dipole-exchange theory. There is also a chapter by Borovik-Romanov and Kreines [40] that reviews light scattering from spin waves, and a review by Grunberg [41] on light scattering from magnetic surface excitations. In particular, we make a comparison between our theory of dipole-exchange frequency dispersion relations and those of Fig. 3 of Ref. [42]. They studied magnon branch crossover by BLS in Fe thin films, which occurs when the surface mode hybridizes with volume waves. We get good agreement with the experimental results of their Fig. 3, taking free boundary conditions and their parameters for an Fe thin film magnetized in-plane, i.e., thickness $2l = 34.3$ nm, $l_{ex} = 3.34$ nm, $H_0 = 2$ kOe, and $4\pi M_s = 21.2$ kOe (propagation is perpendicular to the direction of the magnetization, i.e., $\varphi = \pi/2$).

It is also worth mentioning that Patton [43] has made a good review of the topic of spin-wave modes in ferromagnetic films.

IX. CONCLUSIONS AND SUMMARY

Theoretical results have been presented that allow one to determine with ease the dispersion relations and shapes of the dipole-exchange and magnetostatic modes of a thin ferromagnetic film. In the case of the dipole-exchange modes this involves solving a 6×6 homogeneous matrix eigenvalue problem imposing the determinant to be null, which leads to a nonlinear equation for the eigenfrequencies. The results for the frequency dispersion relations and shapes of the modes are exact, and correspond to uniform magnetic fields applied in an arbitrary direction and boundary conditions that may be quite general at both surfaces of the film. We presented results that compare well with those of previous references, but show some differences in regions of hybridization between modes, regions where our exact treatment should give the right behavior (this was done for boundary conditions of partial pinning associated with uniaxial surface anisotropy of equal value on both surfaces of the film). Also we have shown that the use of approximate dispersion relations for dipole-exchange modes has to be done with care in some cases. An interpretation of the results of the theory is possible; volume modes are explained in terms of the existence of effective purely real wave vectors in the perpendicular direction.

Thus, this theory should be useful for testing experimental results on spin waves in ferromagnetic films, and in particular for testing physical mechanisms that restrict the motion of the magnetization at the surfaces of the film, i.e., different boundary conditions.

ACKNOWLEDGMENTS

This work was supported by Proyecto ICM FP10-061-F-FIC, Chile, and Centers of excellence with BASAL/CONICYT financing, grant FB0807, CEDENNA.

APPENDIX A: THIN FILM MAGNETIZED IN-PLANE

1. Green's functions

In the case of a thin film magnetized in-plane, we will consider three Green's functions, with different associated sources, which in the limits of negligible exchange interaction reproduce a magnetostatic Green's function (case I), and

for negligible magnetostatic interaction reproduce exchange Green's functions (cases II, III).

a. Interior Green's function I

In Fourier space with respect to the z direction (wave vector k), and for $-(k,\omega)$, the magnetostatic equation (18) for the interior Green's function I takes the form

$$\begin{aligned}4\pi\delta(\vec{\rho}-\vec{\rho}') &= -\nabla_\perp^2\phi_I^{-(k,\omega)} + k^2\phi_I^{-(k,\omega)} \\ &\quad + \frac{1}{2}\left[\left(\frac{\partial}{\partial x} - i\frac{\partial}{\partial y}\right)M_+^I + \left(\frac{\partial}{\partial x} + i\frac{\partial}{\partial y}\right)M_-^I\right]. \quad \text{(A1)}\end{aligned}$$

Outside the singularity, the associated Landau-Lifshitz equations (19) are

$$0 = [d(\nabla_\perp^2 - k^2) - h + \Omega]M_+^I + h_+^I, \quad \text{(A2)}$$

$$0 = [d(\nabla_\perp^2 - k^2) - h - \Omega]M_-^I + h_-^I, \quad \text{(A3)}$$

with $h_\pm = -\partial\phi/\partial x \mp i\,\partial\phi/\partial y$, and $h \equiv H_o/4\pi M_s$. Solutions to Eqs. (A1), (A2), (A3) with the right singular behavior take the forms

$$\phi_I^{-(k,\omega)} = CK_0(\beta_I\rho), \quad \text{(A4)}$$

$$M_\pm^{-(k,\omega)} = K_\pm e^{\pm i\theta}K_1(\beta_I\rho), \quad \text{(A5)}$$

with $K_{0,1}$ modified Bessel functions, and (ρ,θ) defined now as polar coordinates measured with respect to the singular point $\vec{\rho}'$. Notice that $(\partial/\partial x \pm i\partial/\partial y)K_0(\beta\rho) = e^{\pm i\theta}[\partial/\partial\rho \pm (i/\rho)\partial/\partial\theta]K_0(\beta\rho) = -\beta e^{\pm i\theta}K_1(\beta\rho)$. The constants C, β_I are obtained by replacing these solutions in the previous equations, leading to

$$\begin{aligned}C &= 2\beta_I^2/k^2, \\ K_\pm &= -\beta_I C/\left[d\left(\beta_I^2 - k^2\right) - h \pm \Omega\right] \equiv \beta_I C k_\pm, \quad \text{(A6)}\end{aligned}$$

with β_I^2 satisfying

$$\frac{2\left(\beta_I^2 - k^2\right)}{\beta_I^2} = \frac{1}{d\left(\beta_I^2 - k^2\right) - h + \Omega} + \frac{1}{d\left(\beta_I^2 - k^2\right) - h - \Omega}, \quad \text{(A7)}$$

i.e., a cubic equation in β_I^2, or

$$\begin{aligned}0 &= \{[d(\beta^2 - k^2) - h]^2 - \Omega^2\}(-\beta^2 + k^2) \\ &\quad + g\beta^2[d(\beta^2 - k^2) - h], \quad \text{(A8)}\end{aligned}$$

where an artificial factor g has been introduced, that is in general 1, but when $g = 0$ it amounts to decoupling the dipolar field. If $\gamma^2 \equiv k^2 - \beta^2$ the previous equation is equivalent to

$$0 = [(h + d\gamma^2)^2 - \Omega^2]\gamma^2 - g(k^2 - \gamma^2)(h + d\gamma^2). \quad \text{(A9)}$$

Defining $d\gamma^2 \equiv \bar{\gamma}^2$ and $dk^2 \equiv \bar{k}^2$ (i.e., measuring lengths in terms of the exchange length, which is done in the numerical calculations), then Eq. (A9) becomes

$$\begin{aligned}0 &= (\bar{\gamma}^2)^3 + 2(h + g/2)(\bar{\gamma}^2)^2 \\ &\quad + (h^2 + gh - g\bar{k}^2 - \Omega^2)\bar{\gamma}^2 - gh\bar{k}^2. \quad \text{(A10)}\end{aligned}$$

This Green's function I corresponds to the "magnetostatic" Green's function since for no exchange ($d = 0$) the differential equation left is [Eqs. (A2), (A3) in (A1) with $d = 0$]

$$4\pi\delta(\vec{\rho} - \vec{\rho}') = -\mu_1(\Omega)\nabla_\perp^2\phi_I^{-(k,\omega)} + k^2\phi_I^{-(k,\omega)}, \quad \text{(A11)}$$

with $\mu_1(\Omega) \equiv [h(h+1) - \Omega^2]/(h^2 - \Omega^2)$, which is the appropriate Green's function equation for the magnetostatic problem. Indeed for $d = 0$ from Eq. (A8) one gets $\beta^2 = k^2/\mu_1(\Omega)$, which corresponds to the right magnetostatic solution. Thus, of the three solutions for β^2 of the cubic equation (A8), β_I^2 should be chosen to approach the limit $k^2/\mu_1(\Omega)$ when $d \to 0$.

Returning to the dipole-exchange case, if $\beta_I^2 = -\kappa_I^2 < 0$, this Green's function takes the form

$$\phi_I^{-(k,\omega)} = \tilde{C}H_0^{(1)}(\kappa_I\rho), \quad \text{(A12)}$$

$$M_\pm^{-(k,\omega)} = \tilde{K}_\pm e^{\pm i\theta}H_1^{(1)}(\kappa_I\rho), \quad \text{(A13)}$$

with $H_{0,1}^{(1)}$ Hankel's functions of type (1):

$$\begin{aligned}-\kappa e^{\pm i\phi}H_1^{(1)}(\kappa\rho) &= (\partial/\partial x \pm i\partial/\partial y)H_0^{(1)}(\beta\rho) \\ &= e^{\pm i\theta}[\partial/\partial\rho \pm (i/\rho)\partial/\partial\theta]H_0^{(1)}(\beta\rho), \quad \text{(A14)}\end{aligned}$$

and the associated constants are

$$\tilde{C} = \pi\kappa_I^2/k^2, \quad \tilde{K}_\pm = \kappa_I\tilde{C}/\left[d\left(\kappa_I^2 + k^2\right) + h \mp \Omega\right] \equiv \kappa_I\tilde{C}\tilde{k}_\pm. \quad \text{(A15)}$$

In Fourier space, for $\beta^2 = \beta_I^2 > 0$ and normalized by πC [$s \equiv \mathrm{sgn}(y - y')$],

$$\phi_I^{-(\vec{Q},\omega)} = e^{-\sqrt{\beta^2+q^2}|y-y'|}/\sqrt{\beta^2 + q^2}, \quad \text{(A16)}$$

$$M_\pm^{-(\vec{Q},\omega)I} = ik_\pm e^{-\sqrt{\beta^2+q^2}|y-y'|}(q/\sqrt{\beta^2 + q^2} \pm s). \quad \text{(A17)}$$

And, for $\beta^2 = -\kappa_I^2 < 0$, normalized by $(-2i)\tilde{C}$, and for $q^2 \geqslant \kappa^2$,

$$\phi_I^{-(\vec{Q},\omega)} = e^{-\sqrt{q^2-\kappa^2}|y-y'|}/\sqrt{q^2 - \kappa^2}, \quad \text{(A18)}$$

$$M_\pm^{-(\vec{Q},\omega)I} = i\tilde{k}_\pm e^{-\sqrt{q^2-\kappa^2}|y-y'|}(q/\sqrt{q^2 - \kappa^2} \pm s). \quad \text{(A19)}$$

For $q^2 < \kappa^2$ in these previous expressions one should replace $\sqrt{q^2 - \kappa^2}$ with $-i\sqrt{\kappa^2 - q^2}$. This choice of sign assures that $i\pi H_0^{(1)}(\kappa\rho)$ is the Green's function of the problem $(\nabla_\perp^2 + \kappa^2)\psi_G^\omega = -4\pi\delta^{(2)}(\rho)$ that has associated outgoing waves, with time dependence $\exp(-i\omega t)$; i.e., it satisfies causality (see Ref. [44]).

b. Interior Green's function II

For $-(k,\omega)$ this Green's function satisfies

$$4\pi\delta(\vec{\rho} - \vec{\rho}') = [d(\nabla_\perp^2 - k^2) - h + \Omega]M_+^{II} + h_+^{-(k,\omega)} \quad \text{(A20)}$$

and out of the singularity:

$$0 = -\nabla_\perp^2 \phi_{II}^{-(k,\omega)} + k^2 \phi_{II}^{-(k,\omega)} + \frac{1}{2}\left[\left(\frac{\partial}{\partial x} - i\frac{\partial}{\partial y}\right)M_+^{II} + \left(\frac{\partial}{\partial x} + i\frac{\partial}{\partial y}\right)M_-^{II}\right], \quad \text{(A21)}$$

$$0 = [d(\nabla_\perp^2 - k^2) - h - \Omega]M_-^{II} + h_-^{-(k,\omega)}. \quad \text{(A22)}$$

Solutions to these equations are

$$\phi_{II}^{-(k,\omega)} = Ee^{-i\theta}K_1(\beta_{II}\rho), \quad \text{(A23)}$$

$$M_+^{II} = DK_0(\beta\rho), \quad \text{(A24)}$$

$$M_-^{II} = Fe^{-i2\theta}K_2(\beta\rho), \quad \text{(A25)}$$

with

$$D = -2\beta_{II}^2/(dk^2 + h - \Omega), \quad \text{(A26)}$$

$$E = -D[d(\beta^2 - k^2) - h + \Omega]/\beta_{II} \equiv D\beta\bar{e}, \quad \text{(A27)}$$

$$F = D\frac{d\left(\beta_{II}^2 - k^2\right) - h + \Omega}{d\left(\beta_{II}^2 - k^2\right) - h - \Omega} = D\left\{-1 + 2\left(\beta_{II}^2 - k^2\right)\left[d\left(\beta_{II}^2 - k^2\right) - h + \Omega\right]/\beta_{II}^2\right\} \equiv D\beta^2 f, \quad \text{(A28)}$$

with β_{II}^2 also satisfying Eq. (A8) [use was made of Eq. (A7)].

This Green's function corresponds to an "exchange" Green's function since decoupling the dipolar term ($g = 0$) from Eq. (A8) one gets

$$\beta_{II}^2 = k^2 + (h - \Omega)/d; \quad \text{(A29)}$$

i.e., one should take β_{II}^2 as the solution of Eq. (A8) which tends to $\beta_{II}^2 = k^2 + (h - \Omega)/d$ as $g \to 0$.

If $\beta_{II}^2 = -\kappa_{II}^2 < 0$, this Green's function takes the form

$$\phi_{II}^{-(k,\omega)} = \tilde{E}e^{-i\theta}H_1^{(1)}(\kappa_{II}\rho), \quad \text{(A30)}$$

$$M_+^{-(k,\omega)II} = \tilde{D}H_0^{(1)}(\kappa_{II}\rho), \quad \text{(A31)}$$

$$M_-^{-(k,\omega)II} = \tilde{F}e^{-2i\theta}H_2^{(1)}(\kappa_{II}\rho), \quad \text{(A32)}$$

with

$$\tilde{D} = i\pi\kappa_{II}^2/(dk^2 + h - \Omega), \quad \text{(A33)}$$

$$\tilde{E} = -\tilde{D}\left[d\left(\kappa_{II}^2 + k^2\right) + h - \Omega\right]/\kappa_{II} \equiv \tilde{D}\kappa\tilde{e}, \quad \text{(A34)}$$

$$\tilde{F} = -\tilde{D}\frac{d\left(\kappa_{II}^2 + k^2\right) + h - \Omega}{d\left(\kappa_{II}^2 + k^2\right) + h + \Omega} = \tilde{D}\left\{1 + 2\left(\kappa_{II}^2 + k^2\right)\left[d\left(\kappa_{II}^2 + k^2\right) + h - \Omega\right]/\kappa_{II}^2\right\} \equiv \tilde{D}\kappa^2\tilde{f}. \quad \text{(A35)}$$

In Fourier space, for $\beta^2 = \beta_{II}^2 > 0$ and normalized by πD,

$$\phi_{II}^{-(\vec{Q},\omega)} = i\bar{e}e^{-\sqrt{\beta^2+q^2}|y-y'|}(q/\sqrt{\beta^2+q^2} - s), \quad \text{(A36)}$$

$$M_+^{-(\vec{Q},\omega)II} = e^{-\sqrt{\beta^2+q^2}|y-y'|}/\sqrt{\beta^2+q^2}, \quad \text{(A37)}$$

$$M_-^{-(\vec{Q},\omega)II} = -fe^{-\sqrt{\beta^2+q^2}|y-y'|}(q^2/\sqrt{\beta^2+q^2} - 2qs + \sqrt{\beta^2+q^2}). \quad \text{(A38)}$$

And, for $\beta^2 = -\kappa_{II}^2 < 0$, $q^2 \geqslant \kappa_{II}^2$, and normalized by $(-2i)\tilde{D}$,

$$\phi_{II}^{-(\vec{Q},\omega)} = i\tilde{e}e^{-\sqrt{q^2-\kappa^2}|y-y'|}(q/\sqrt{q^2-\kappa^2} - s), \quad \text{(A39)}$$

$$M_+^{-(\vec{Q},\omega)II} = e^{-\sqrt{q^2-\kappa^2}|y-y'|}/\sqrt{q^2-\kappa^2}, \quad \text{(A40)}$$

$$M_-^{-(\vec{Q},\omega)II} = -\tilde{f}e^{-\sqrt{q^2-\kappa^2}|y-y'|}(q^2/\sqrt{q^2-\kappa^2} - 2qs + \sqrt{q^2-\kappa^2}). \quad \text{(A41)}$$

For $q^2 < \kappa_{II}^2$ one should replace everywhere $\sqrt{q^2-\kappa^2}$ with $-i\sqrt{\kappa^2-q^2}$. This follows from the mentioned prescription for $H_0^{(1)}(\kappa\rho)$, which applies also to the functions $e^{\pm i\theta}H_1^{(1)}(\kappa\rho)$ and $e^{\pm i2\theta}H_2^{(1)}(\kappa\rho)$ since those follow as derivatives of $H_0^{(1)}(\kappa\rho)$, i.e., with Fourier transforms simply related.

c. Interior Green's function III

For $-(k,\omega)$ this Green's function satisfies

$$4\pi\delta(\vec{\rho} - \vec{\rho}') = [d(\nabla_\perp^2 - k^2) - h - \Omega]M_-^{III} + h_-^{-(k,\omega)}. \quad \text{(A42)}$$

And out of the singularity,

$$0 = -\nabla_\perp^2 \phi_{III}^{-(k,\omega)} + k^2 \phi_{III}^{-(k,\omega)} + \frac{1}{2}\left[\left(\frac{\partial}{\partial x} - i\frac{\partial}{\partial y}\right)M_+^{III} + \left(\frac{\partial}{\partial x} + i\frac{\partial}{\partial y}\right)M_-^{III}\right], \quad \text{(A43)}$$

$$0 = [d(\nabla_\perp^2 - k^2) - h + \Omega]M_+^{III} + h_+^{-(k,\omega)}. \quad \text{(A44)}$$

Solutions to these equations are

$$\phi_{III}^{-(k,\omega)} = He^{i\theta}K_1(\beta_{III}\rho), \quad \text{(A45)}$$

$$M_-^{III} = GK_0(\beta_{III}\rho), \quad \text{(A46)}$$

$$M_+^{III} = Je^{i2\theta}K_2(\beta_{III}\rho), \quad \text{(A47)}$$

with

$$G = -2\beta_{III}^2/(dk^2 + h + \Omega), \quad \text{(A48)}$$

$$H = -G\left[d\left(\beta_{III}^2 - k^2\right) - h - \Omega\right]/\beta_{III} \equiv G\beta_{III}\bar{h}, \quad \text{(A49)}$$

$$J = G\frac{d\left(\beta_{III}^2 - k^2\right) - h - \Omega}{d\left(\beta_{III}^2 - k^2\right) - h + \Omega} = G\left\{-1 + 2\left(\beta_{III}^2 - k^2\right)\left[d\left(\beta_{III}^2 - k^2\right) - h - \Omega\right]/\beta_{III}^2\right\} \equiv G\beta_{III}^2 j, \quad \text{(A50)}$$

with β_{III}^2 also satisfying Eq. (A8).

This Green's function corresponds to an "exchange" Green's function since decoupling the dipolar term ($g = 0$) one gets

$$\beta_{III}^2 = k^2 + (h + \Omega)/d. \quad \text{(A51)}$$

For $\beta_{III}^2 = -\kappa_{III}^2 < 0$,

$$\phi_{III}^{-(k,\omega)} = \tilde{H} e^{i\phi} H_1^{(1)}(\kappa_{III}\rho), \tag{A52}$$

$$M_-^{III} = \tilde{G} H_0^{(1)}(\kappa_{III}\rho), \tag{A53}$$

$$M_+^{III} = \tilde{J} e^{i2\phi} H_2^{(1)}(\kappa_{III}\rho), \tag{A54}$$

with

$$\tilde{G} = i\pi\kappa_{III}^2/(dk^2 + h + \Omega), \tag{A55}$$

$$\tilde{H} = -\tilde{G}\big[d\big(\kappa_{III}^2 + k^2\big) + h + \Omega\big]/\kappa_{III} \equiv \tilde{G}\kappa_{III}\tilde{h}, \tag{A56}$$

$$\begin{aligned}\tilde{J} &= -\tilde{G}\frac{d\big(\kappa_{III}^2 + k^2\big) + h + \Omega}{d\big(\beta_{III}^2 + k^2\big) + h - \Omega} \\ &= \tilde{G}\big\{1 + 2\big(\kappa_{III}^2 + k^2\big)\big[d\big(\kappa_{III}^2 + k^2\big) + h + \Omega\big]/\kappa_{III}^2\big\} \\ &\equiv \tilde{G}\kappa_{III}^2\tilde{j}.\end{aligned} \tag{A57}$$

In Fourier space, for $\beta^2 = \beta_{III}^2 > 0$ and normalized by πG,

$$\phi_{III}^{-(\vec{Q},\omega)} = i\tilde{h} e^{-\sqrt{\beta^2+q^2}|y-y'|}(q/\sqrt{\beta^2+q^2} + s), \tag{A58}$$

$$\begin{aligned}M_+^{-(\vec{Q},\omega)III} &= -je^{-\sqrt{\beta^2+q^2}|y-y'|}(q^2/\sqrt{\beta^2+q^2} + 2qs \\ &\quad + \sqrt{\beta^2+q^2}),\end{aligned} \tag{A59}$$

$$M_-^{-(\vec{Q},\omega)III} = e^{-\sqrt{\beta^2+q^2}|y-y'|}/\sqrt{\beta^2+q^2}. \tag{A60}$$

And, for $\beta^2 = -\kappa_{III}^2 < 0$, $q^2 \geqslant \kappa_{III}^2$, and normalized by $(-2i)\tilde{G}$,

$$\phi_{III}^{-(\vec{Q},\omega)} = i\tilde{h} e^{-\sqrt{q^2-\kappa^2}|y-y'|}(q/\sqrt{q^2-\kappa^2} + s), \tag{A61}$$

$$\begin{aligned}M_+^{-(\vec{Q},\omega)III} &= -\tilde{j}e^{-\sqrt{q^2-\kappa^2}|y-y'|}(q^2/\sqrt{q^2-\kappa^2} + 2qs \\ &\quad + \sqrt{q^2-\kappa^2}),\end{aligned} \tag{A62}$$

$$M_-^{-(\vec{Q},\omega)III} = e^{-\sqrt{q^2-\kappa^2}|y-y'|}/\sqrt{q^2-\kappa^2}. \tag{A63}$$

For $q^2 < \kappa_{III}^2$ one should replace everywhere $\sqrt{q^2-\kappa^2}$ with $-i\sqrt{\kappa^2-q^2}$.

APPENDIX B: THIN FILM MAGNETIZED AT AN ANGLE FROM ITS PLANE

1. Green's functions

The equations to be solved for the Green's functions in the case of an applied magnetic field at an angle with the plane of the film are [they follow from Eqs. (18), (19), and are written in Fourier space, for components $-(\vec{Q},\omega)$, $h_i \equiv H_i/4\pi M_s$, and they are in their homogeneous form, i.e., considered out of the singularity]:

$$\begin{aligned}0 &= \left(-\frac{\partial^2}{\partial y^2} + Q^2\right)\phi_G^{-(\vec{Q},\omega)} \\ &\quad - \frac{i}{2}\left(\cos\theta_M\frac{\partial}{\partial y} + ik\sin\theta_M\right)(M_+^G - M_-^G) \\ &\quad - \frac{i}{2}q(M_+^G + M_-^G),\end{aligned}$$

$$\begin{aligned}0 &= \left[d\left(\frac{\partial^2}{\partial y^2} - Q^2\right) - h_i + \Omega\right]M_+^G \\ &\quad + \left(iq + \sin\theta_M k - i\cos\theta_M\frac{\partial}{\partial y}\right)\phi_G^{-(\vec{Q},\omega)}, \\ 0 &= \left[d\left(\frac{\partial^2}{\partial y^2} - Q^2\right) - h_i - \Omega\right]M_-^G \\ &\quad + \left(iq - \sin\theta_M k + i\cos\theta_M\frac{\partial}{\partial y}\right)\phi_G^{-(\vec{Q},\omega)}.\end{aligned} \tag{B1}$$

Based on our previous solutions for the case of magnetization in-plane ($\theta_M = 0$), for $\theta_M \neq 0$ we look for solutions of the form

$$\phi_G^{-(\vec{Q},\omega)} = Ae^{-\alpha|y-y'|}, \quad M_\pm^G = B_\pm e^{-\alpha|y-y'|}. \tag{B2}$$

Replacing these previous forms into Eqs. (B1) one obtains the following linear system for $A, B_\pm$ [$s \equiv \mathrm{sgn}(y-y')$]:

$$\begin{aligned}0 &= 2(\alpha^2 - Q^2)A + i(q - \alpha s\cos\theta_M + ik\sin\theta_M)B_+ \\ &\quad + i(q + \alpha s\cos\theta_M - ik\sin\theta_M)B_-,\end{aligned} \tag{B3}$$

$$\begin{aligned}0 &= [d(\alpha^2 - Q^2) - h_i + \Omega]B_+ \\ &\quad + i(q + \alpha s\cos\theta_M - ik\sin\theta_M)A,\end{aligned} \tag{B4}$$

$$\begin{aligned}0 &= [d(\alpha^2 - Q^2) - h_i - \Omega]B_- \\ &\quad + i(q - \alpha s\cos\theta_M + ik\sin\theta_M)A.\end{aligned} \tag{B5}$$

Inserting Eqs. (B4) and (B5) into Eq. (B3) leads to the following equation for α:

$$\begin{aligned}2(\alpha^2 - Q^2) &= -[(k\sin\theta_M + i\alpha s\cos\theta_M)^2 + q^2] \\ &\quad \times\left(\frac{1}{d(\alpha^2 - Q^2) - h_i + \Omega}\right. \\ &\quad \left. + \frac{1}{d(\alpha^2 - Q^2) - h_i - \Omega}\right),\end{aligned} \tag{B6}$$

which is equivalent to Eq. (A7) for $\theta_M = 0$ ($\alpha^2 - Q^2 = \beta^2 - k^2 = -\gamma^2$ in that case). For general θ_M the previous Eq. (B6) is a sixth-order equation for α, with different solutions in the regions $(y - y') \gtrless 0$. [Also notice that for $\theta_M = 0$ the Fourier components of the already obtained Green's functions I, II, and III satisfy the homogeneous equations (B3), (B4), and (B5).]

Notice that if the previous equation (B6) for α is written in terms of the variable $iu = \alpha$ it becomes an equation for the roots of a sixth-order polynomial in u with real coefficients: by a theorem of algebra it has solutions that come in complex conjugate pairs. Coming back to the variable α this means that there are three solutions with the real part of α positive, and three solutions with their real parts the negatives of the previous values. For the Green's function solutions (B2) we take the three solutions with real parts of α positive; i.e., they are generalizations of the previous three Green's functions (I, II, III) found in the in-plane case.

Thus, we have three solutions α_j^u [$j = 1,2,3$, with $\mathrm{Re}(\alpha_j^u) \geqslant 0$] corresponding to $y - y' > 0$, each with its

associated constants $A_j^u, B_{j\pm}^u$, that satisfy

$$0 = 2\left[\left(\alpha_j^u\right)^2 - Q^2\right]A_j^u + i\left(q - \alpha_j^u \cos\theta_M + ik\sin\theta_M\right)B_{j+}^u + i\left(q + \alpha_j^u \cos\theta_M - ik\sin\theta_M\right)B_{j-}^u, \tag{B7}$$

$$0 = \left\{d\left[\left(\alpha_j^u\right)^2 - Q^2\right] - h_i + \Omega\right\}B_{j+}^u + i\left(q + \alpha_j^u \cos\theta_M - ik\sin\theta_M\right)A_j^u, \tag{B8}$$

$$0 = \left\{d\left[\left(\alpha_j^u\right)^2 - Q^2\right] - h_i - \Omega\right\}B_{j-}^u + i\left(q - \alpha_j^u \cos\theta_M + ik\sin\theta_M\right)A_j^u, \tag{B9}$$

and with α_j^u satisfying

$$2\left[\left(\alpha_j^u\right)^2 - Q^2\right] = -\left[\left(k\sin\theta_M + i\alpha_j^u\cos\theta_M\right)^2 + q^2\right] \times \left(\frac{1}{d\left[\left(\alpha_j^u\right)^2 - Q^2\right] - h_i + \Omega} + \frac{1}{d\left[\left(\alpha_j^u\right)^2 - Q^2\right] - h_i - \Omega}\right). \tag{B10}$$

The solution to the homogeneous equations (B7), (B8), and (B9) gives the Green's function associated with α_j^u for a given $j = 1,2,3$ (they are arbitrary up to a multiplicative constant: this is not relevant as far as the determination of the frequency dispersion relations); i.e., $A_j^u, B_{j\pm}^u$ are considered to be known from now on. And, we have three solutions α_j^d [$j = 1,2,3$, with $\mathrm{Re}(\alpha_j^d) \geqslant 0$] corresponding to $y - y' < 0$, each with its associated constants $A_j^d, B_{j\pm}^d$, that satisfy

$$0 = 2\left[\left(\alpha_j^d\right)^2 - Q^2\right]A_j^d + i\left(q + \alpha_j^d \cos\theta_M + ik\sin\theta_M\right)B_{j+}^d + i\left(q - \alpha_j^d \cos\theta_M - ik\sin\theta_M\right)B_{j-}^d, \tag{B11}$$

$$0 = \left\{d\left[\left(\alpha_j^d\right)^2 - Q^2\right] - h_i + \Omega\right\}B_{j+}^d + i\left(q - \alpha_j^d \cos\theta_M - ik\sin\theta_M\right)A_j^d, \tag{B12}$$

$$0 = \left\{d\left[\left(\alpha_j^d\right)^2 - Q^2\right] - h_i - \Omega\right\}B_{j-}^d + i\left(q + \alpha_j^d \cos\theta_M + ik\sin\theta_M\right)A_j^d, \tag{B13}$$

and with α_j^d satisfying

$$2\left[\left(\alpha_j^d\right)^2 - Q^2\right] = -\left[\left(k\sin\theta_M - i\alpha_j^d\cos\theta_M\right)^2 + q^2\right] \times \left(\frac{1}{d\left[\left(\alpha_j^d\right)^2 - Q^2\right] - h_i + \Omega} + \frac{1}{d\left[\left(\alpha_j^d\right)^2 - Q^2\right] - h_i - \Omega}\right). \tag{B14}$$

The solutions $A_j^d, B_{j\pm}^d$ to Eqs. (B11), (B12), and (B13) are thus known, except for an overall multiplicative constant.

The prescription is to choose three α_u's and three α_d's with real parts positive, and there is a question about how to choose the solutions that are purely imaginary: the solutions for α_d are the negatives of the ones for α_u, so for purely imaginary roots, of the 6 solutions for α_u one should leave one of the purely imaginary solutions for α_u and the other for α_d (one has to change its sign in the process). At the end the six plane-wave solutions separated into 3 α_u and 3 α_d cases are equivalent to having kept the 6 plane-wave solutions for α_u (as far as the dependence on y).

2. Spin-wave modes

In this section it is explained how to solve for the spin-wave modes inside or outside the film, for an arbitrary direction of the applied magnetic field. Using Eq. (34) in the upper surface of Fig. 2, one obtains

$$\begin{aligned} 0 = {} & \phi(l)\left[b_y^{G_j^u}(l - y') - Q\phi^{G_j^u}(l - y')\right] - \phi(y')b_y^{G_j^u}(0^+) + \phi^{G_j^u}(0^+)b_y(y') \\ & - \frac{d}{2}\left(\frac{\partial M_-}{\partial y}(l)M_+^{G_j^u}(l - y') + \frac{\partial M_+}{\partial y}(l)M_-^{G_j^u}(l - y') - \frac{\partial M_-}{\partial y}(y')M_+^{G_j^u}(0^+) - \frac{\partial M_+}{\partial y}(y')M_-^{G_j^u}(0^+)\right) \\ & + \frac{d}{2}\left(\frac{\partial M_-^{G_j^u}}{\partial y}(l - y')M_+(l) + \frac{\partial M_+^{G_j^u}}{\partial y}(l - y')M_-(l) - \frac{\partial M_-^{G_j^u}}{\partial y}(0^+)M_+(y') - \frac{\partial M_+^{G_j^u}}{\partial y}(0^+)M_-(y')\right), \end{aligned} \tag{B15}$$

where according to Eqs. (24)

$$\phi^{G_j^u}(0^+) = A_j^u, \quad b_y^{G_j^u}(0^+) = \alpha_j^u A_j^u - (i/2)\left(B_{+j}^u - B_{-j}^u\right), \quad M_\pm^{G_j^u}(0^+) = B_{\pm j}^u, \quad \partial M_\pm^{G_j^u}/\partial y(0^+) = -\alpha_j^u B_{\pm j}^u; \tag{B16}$$

i.e., they are known quantities (see the previous section). Also, using Eq. (34) in the lower surface of Fig. 2, one obtains

$$\begin{aligned} 0 = {} & -\phi(-l)\left[b_y^{G_j^d}(-l - y') + Q\phi^{G_j^d}(-l - y')\right] + \phi(y')b_y^{G_j^d}(0^-) - \phi^{G_j^d}(0^-)b_y(y') \\ & + \frac{d}{2}\left(\frac{\partial M_-}{\partial y}(-l)M_+^{G_j^d}(-l - y') + \frac{\partial M_+}{\partial y}(-l)M_-^{G_j^d}(-l - y') - \frac{\partial M_-}{\partial y}(y')M_+^{G_j^d}(0^-) - \frac{\partial M_+}{\partial y}(y')M_-^{G_j^d}(0^-)\right) \\ & - \frac{d}{2}\left(\frac{\partial M_-^{G_j^d}}{\partial y}(-l - y')M_+(-l) + \frac{\partial M_+^{G_j^d}}{\partial y}(-l - y')M_-(-l) - \frac{\partial M_-^{G_j^d}}{\partial y}(0^-)M_+(y') - \frac{\partial M_+^{G_j^d}}{\partial y}(0^-)M_-(y')\right), \end{aligned} \tag{B17}$$

where from Eqs. (24)

$$\phi^{G_j^d}(0^-) = A_j^d, \quad b_y^{G_j^d}(0^-) = -\alpha_j^d A_j^d - (i/2)\left(B_{+j}^d - B_{-j}^d\right),$$

$$M_\pm^{G_j^d}(0^-) = B_{\pm j}^d, \quad \partial M_\pm^{G_j^d}/\partial y(0^-) = \alpha_j^d B_{\pm j}^d; \tag{B18}$$

i.e., they are known quantities (previous section).

Equations (B15) and (B17) correspond to 6 equations ($j = 1,2,3$) for 6 unknowns:

$$\phi(y'), \quad b_y(y'), \quad M_\pm(y'), \quad \partial M_\pm/\partial y(y'); \tag{B19}$$

i.e., they allow one to determine these quantities for arbitrary y' or equivalently the spin-wave modes inside the sample.

Similarly one can obtain the modes out of the thin film. For example in the upper region, one can consider two analogous surfaces over and below a point y' ($y' > l$), leading to the following two equations for the two unknowns $\phi(y'), b_y(y')$:

$$0 = -\phi(y')b_y^0(0^+) + b_y(y')\phi^0(0^+), \tag{B20}$$

$$0 = \phi(y')b_y^0(0^-) - b_y(y')\phi^0(0^-) - \phi(l)b_y^0(l-y') + \phi^0(l-y')b_y(l). \tag{B21}$$

3. Ultrathin-film limit

In the ultrathin-film limit, i.e., when the thickness of the film is of the order of the exchange length $l_{ex} = \sqrt{D/4\pi M_s}$, a good approximation is to consider that the magnetization is uniform over the thickness of the film. Then the Landau-Lifshitz equations (9) for the modes are driven by the dipolar fields averaged over the film thickness (among other fields). Using the variables $M_\pm \equiv 4\pi(m_x \pm i m_{\tilde{y}})$, these equations become

$$\Omega M_+ = d\nabla^2 M_+ + \langle H_x + i H_{\tilde{y}}\rangle - h_i M_+, \tag{B22}$$

$$\Omega M_- = -d\nabla^2 M_- - \langle H_x - i H_{\tilde{y}}\rangle + h_i M_-, \tag{B23}$$

with $\Omega \equiv \omega/(|\gamma|4\pi M_s)$, $d = l_{ex}^2 = D/4\pi M_s$, $h_i = H_i/4\pi M_s$. The magnetostatic potential satisfies Eq. (6), which in this case takes the form

$$-\partial^2\phi/\partial y^2 + Q^2\phi = -\tfrac{1}{2}[(iq - k\sin\theta_M)M_+ + (iq + k\sin\theta_M)M_-] \tag{B24}$$

with $k = Q\cos\varphi$ and $q = Q\sin\varphi$. The solution to Eq. (B24) for the potential takes the following forms over, inside, and below the film, respectively:

$$\phi(\vec{x}) = e^{i\vec{Q}\cdot\vec{x}}\begin{cases} Ue^{-Q(y-l)}, \\ a\cosh(Qy) + b\sinh(Qy) - \frac{1}{2Q}[(i\sin\varphi - \cos\varphi\sin\theta_M)M_+ + (i\sin\varphi + \cos\varphi\sin\theta_M)M_-], \\ Le^{Q(y+l)}. \end{cases} \tag{B25}$$

One obtains the unknown constants U,a,b,L by imposing the boundary conditions of continuous potential and normal magnetic induction on the surfaces of the films. Then, the dipolar fields follow by simple differentiation of the just found magnetostatic potential, and their averaged values over the thickness of the film are

$$\langle H_x \pm i H_{\tilde{y}}\rangle = -\frac{1}{2}\left[1 - \frac{(1-e^{-2Ql})}{2Ql}\right][(\sin\varphi + i\cos\varphi\sin\theta_M)M_+ + (\sin\varphi - i\cos\varphi\sin\theta_M)M_-](\sin\varphi \mp i\cos\varphi\sin\theta_M) \mp \frac{1}{2}\cos^2\theta_M(M_+ - M_-)\frac{(1-e^{-2Ql})}{2Ql}. \tag{B26}$$

Now, since in this approximation $\nabla^2 M_\pm = -Q^2 M_\pm$, Eqs. (B23) become a simple linear eigenvalue problem, and the corresponding frequency dispersion relation in the ultrathin-film limit satisfies

$$\Omega^2 = (hi + dQ^2)^2 + \left[(\sin^2\varphi + \cos^2\varphi\sin^2\theta_M)\left(1 - \frac{(1-e^{-2Ql})}{2Ql}\right) + \cos^2\theta_M\frac{(1-e^{-2Ql})}{2Ql}\right](hi + dQ^2) + \sin^2\varphi\cos^2\theta_M\left(1 - \frac{(1-e^{-2Ql})}{2Ql}\right)\frac{(1-e^{-2Ql})}{2Ql}. \tag{B27}$$

The case magnetized in-plane, i.e., $\theta_M = 0$ ($h_i = h$), becomes

$$\Omega^2 = \left[h + dQ^2 + \sin^2\varphi\left(1 - \frac{(1-e^{-2Ql})}{2Ql}\right)\right]\left[h + dQ^2 + \frac{(1-e^{-2Ql})}{2Ql}\right]. \tag{B28}$$

And the case magnetized perpendicular to the plane, i.e., $\theta_M = \pi/2$, becomes

$$\Omega^2 = [h - 1 + dQ^2]\left[h + dQ^2 - \frac{(1-e^{-2Ql})}{2Ql}\right], \tag{B29}$$

in this case $h_i = h - 1$.

4. Magnetostatic extinction equations

The following magnetostatic extinction equations allow one to calculate the dispersion relations of magnetostatic modes in ferromagnetic fields under an applied magnetic field that is inclined at an angle θ_H from the plane (also they allow one to determine the modes evaluated on the surfaces of the film,

and if needed the modes can be determined everywhere by a procedure analogous to the one used for dipole-exchange modes). These equations follow from Eqs. (45) and (46) by discarding the terms proportional to the exchange interaction:

$$0 = e^{-\alpha_j^u l}\left[2\left(\alpha_j^u - Q\right) - \cos\theta_M\left(b_{j+}^u - b_{j-}^u\right)\right]\phi(l) - e^{\alpha_j^u l}\left[2\left(\alpha_j^u + Q\right) - \cos\theta_M\left(b_{j+}^u - b_{j-}^u\right)\right]\phi(-l), \quad \text{(B30)}$$

$$0 = -e^{\alpha_j^d l}\left[2\left(\alpha_j^d + Q\right) + \cos\theta_M\left(b_{j+}^d - b_{j-}^d\right)\right]\phi(l) + e^{-\alpha_j^d l}\left[2\left(\alpha_j^d - Q\right) + \cos\theta_M\left(b_{j+}^d - b_{j-}^d\right)\right]\phi(-l), \quad \text{(B31)}$$

with

$$b_+^u = -(q + \alpha_u\cos\theta_M - ik\sin\theta_M)/(h_i - \Omega), \quad \text{(B32)}$$

$$b_-^u = -(q - \alpha_u\cos\theta_M + ik\sin\theta_M)/(h_i + \Omega), \quad \text{(B33)}$$

$$b_+^d = -(q - \alpha_d\cos\theta_M - ik\sin\theta_M)/(h_i - \Omega), \quad \text{(B34)}$$

$$b_-^d = -(q + \alpha_d\cos\theta_M + ik\sin\theta_M)/(h_i + \Omega), \quad \text{(B35)}$$

and the parameters $\alpha^{u,d}$ satisfy the following equations that follow from Eqs. (B10) and (B14) when $d \to 0$:

$$0 = \alpha_u^2 - Q^2 - h_i[q^2 + (k\sin\theta_M + i\alpha_u\cos\theta_M)^2]/\left(h_i^2 - \Omega^2\right), \quad \text{(B36)}$$

$$0 = \alpha_d^2 - Q^2 - h_i[q^2 + (k\sin\theta_M - i\alpha_d\cos\theta_M)^2]/\left(h_i^2 - \Omega^2\right), \quad \text{(B37)}$$

with θ_M determined by solving Eq. (1).

Thus, replacing Eqs. (B32)–(B37) in Eqs. (B30) and (B31), one obtains the dispersion relations by imposing that the determinant of the corresponding 2×2 matrix to be null. The potentials evaluated at the surfaces follow from Eqs. (B30) and (B31) once the frequencies have been determined; i.e., they correspond to the eigenvectors.

[1] R. W. Damon and J. R. Eshbach, J. Phys. Chem. Solids **19**, 308 (1961).
[2] M. J. Hurben and C. E. Patton, J. Magn. Magn. Mater. **139**, 263 (1995).
[3] Z. Z. Dhong, in *Handbook of Thin Film Materials*, Vol. 5 (Academic Press, San Diego, 2002), Chap. 4.
[4] B. A. Kalinikos, in *Linear and Nonlinear Spin Waves in Magnetic Films and Superlattices*, edited by M. G. Cottam (World Scientific, Singapore, 1994), Chap. 2.
[5] V. V. Gann, Sov. Phys. Solid State **8**, 2537 (1967).
[6] T. Wolfram and R. E. De Wames, Phys. Lett. A **30**, 2 (1969).
[7] R. E. De Wames and T. Wolfram, Appl. Phys. Lett. **15**, 297 (1969).
[8] R. E. De Wames and T. Wolfram, J. Appl. Phys. **41**, 987 (1970).
[9] T. Wolfram and R. E. De Wames, Phys. Rev. Lett. **24**, 1489 (1970).
[10] M. Sparks, Phys. Rev. B **1**, 3831 (1970).
[11] B. N. Filippov, Phys. Met. Metallogr. **32**, 911 (1971).
[12] B. N. Filippov and I. G. Titjakov, Phys. Met. Metallogr. **35**, 28 (1973).
[13] L. V. Mikhailovskaya and R. G. Khlebopros, Sov. Phys. Solid State **16**, 46 (1974).
[14] Yu. V. Gulyaev, P. E. Zil'berman, and A. V. Lugovskoi, Sov. Phys. Solid State **23**, 660 (1981).
[15] A. V. Lugovskoi and P. E. Zil'berman, Sov. Phys. Solid State **24**, 259 (1982).
[16] O. G. Vendik and D. N. Chartorizhskii, Sov. Phys. Solid State **12**, 1209 (1970).
[17] O. G. Vendik, B. A. Kalinikos, and D. N. Chartorizhskii, Sov. Phys. Solid State **16**, 1785 (1975).
[18] B. A. Kalinikos, Sov. Phys. **24**, 719 (1981).
[19] B. A. Kalinikos and A. N. Slavin, J. Phys. C: Solid State Phys. **19**, 7013 (1986).
[20] B. A. Kalinikos, J. Phys.: Condens. Matter **2**, 9861 (1990).
[21] M. Kostylev, J. Appl. Phys. **113**, 053907 (2013).
[22] M. P. Kostylev, B. A. Kalinikos, and H. Dotsch, J. Magn. Magn. Mater. **145**, 93 (1995).
[23] R. F. Soohoo, Phys. Rev. **131**, 594 (1963).
[24] R. Magaraggia, K. Kennewell, M. Kostylev, R. L. Stamps, M. Ali, D. Greig, B. J. Hickey, and C. H. Marrows, Phys. Rev. B **83**, 054405 (2011).
[25] M. Kostylev, J. Appl. Phys. **115**, 233902 (2014).
[26] G. T. Rado and J. R. Weertman, J. Phys. Chem. Solids **11**, 315 (1959).
[27] A. G. Gurevich and G. A. Melkov, *Magnetization Oscillations and Waves* (CRC Press, Boca Raton, 1996).
[28] R. E. Arias, IEEE Magn. Lett. **6**, 3200304 (2015).
[29] M. H. Seavey Jr. and P. E. Tannenwald, Phys. Rev. Lett. **1**, 168 (1958).
[30] C. Kittel, Phys. Rev. **110**, 1295 (1958).
[31] G. I. Lykken, Phys. Rev. Lett. **19**, 1431 (1967).
[32] Z. Frait, Phys. Status Solidi **2**, 1417 (1962).
[33] R. Weber, IEEE Trans. Magn. **4**, 28 (1968).
[34] H. Puszkarski, Acta Phys. Pol. A **38**, 217 (1970).
[35] H. Puszkarski, Acta Phys. Pol. A **38**, 889 (1970).
[36] P. E. Wigen, T. S. Stakelon, H. Puszkarski, and P. Yen, in *Magnetism and Magnetic Materials*, edited by J. J. Becker, G. H. Lander and J. J. Rhyne, AIP Conf. Proc. No. 29 (AIP, New York, 1976), p. 670.
[37] I. S. Maksymov and M. Kostylev, Physica E **69**, 253 (2015).
[38] V. V. Matyushev, M. P. Kostylev, A. A. Stashkevich, and J. M. Desvignes, J. Appl. Phys. **77**, 2087 (1995).
[39] J. R. Dutcher, in *Linear and Nonlinear Spin Waves in Magnetic Films and Superlattices*, edited by M. G. Cottam (World Scientific, Singapore, 1994), Chap. 6.
[40] A. S. Borovik-Romanov and N. M. Kreines, in *Spin Waves and Magnetic Excitations*, Modern Problems in Condensed Matter Sciences, Vol. 22, edited by V. M. Agranovich and A. A. Maradudin (North-Holland, Amsterdam, 1988), Chap. 2.
[41] P. A. Grunberg, Prog. Surf. Sci. **18**, 1 (1985).
[42] P. Kabos, W. D. Wilber, C. E. Patton, and P. Grunberg, Phys. Rev. B **29**, 6396(R) (1984).
[43] C. E. Patton, Phys. Rep. **103**, 251 (1984).
[44] R. Toscano Couto, Revista Brasileira de Ensino de Física **35**, 1304 (2013).